

Arkansas Nuclear One - Unit 2

CEN-214(A)-NP

CETOP-D Code Structure and
Modeling Methods for
Arkansas Nuclear One - Unit 2

July 1982

Combustion Engineering, Inc.
Nuclear Power Systems
Windsor, CT

8209210 178

LEGAL NOTICE

This report was prepared as an account of work sponsored by Combustion Engineering, Inc. Neither Combustion Engineering nor any person acting on its behalf:

A. Makes any warranty or representation, express or implied including the warranties of fitness for a particular purpose or merchantability, with respect to the accuracy, completeness, or usefulness of the information contained in this report, or that the use of any information, apparatus, method, or process disclosed in this report may not infringe privately owned rights; or

B. Assumes any liabilities with respect to the use of, or for damages resulting from the use of, any information, apparatus, method or process disclosed in this report.

ABSTRACT

The CETOP-D Computer Code has been developed for determining core thermal margins for C-E reactors. It uses the same conservation equations as used in the TORC code (Reference 1) for predicting the CE-1 minimum DNBR (MDNBR) in its 4-channel core representation.

The CETOP-D model to be presented in this report differs from the TORC design model (described in Reference 5 and referred to herein as S-TORC, for "Simplified" TORC) by its simpler geometry (four flow channels) yet faster calculation algorithm (prediction-correction method). S-TORC utilizes the comparatively less efficient iteration method on a typical 20-channel geometry.

To produce a design thermal margin model for a specific core, either S-TORC or CETOP-D is benchmarked against a multi-stage TORC model (Detailed TORC described in Reference 1) which is a detailed three-dimensional description of the core thermal hydraulics.

In this report, the CETOP-D and Detailed TORC predicted hot channel MDNBR's are compared, within design operating ranges, for the C-E ANO-2, cycle 2 reactor core, comprised of 16x16 fuel assemblies. Results, in terms of deviation between each pair of MDNBR's predicted by the two models, show that CETOP-D with the inclusion of the "adjusted" hot assembly flow factor, can predict either conservative or accurate MDNBR's, compared with Detailed TORC.

Reference 17 was provided to NRC in support of the use of CETOP-D for the ANO-2 Cycle 2 reload analysis. The use of CETOP-D for ANO-2 was accepted by NRC in Reference 18.

This document is a revised version of Reference 17 correcting typographical errors and incorporating other changes identified during the review for ANO-2 Cycle 2. It is being reissued as an independent document for reference purposes. Changes from Reference 17 are identified with vertical lines in the right hand margin. Additional information on CETOP-D in the form of responses to NRC questions can be found in Reference 19.

TABLE OF CONTENTS

<u>Section</u>	<u>Title</u>	<u>Page</u>
	ABSTRACT	i
	TABLE OF CONTENTS	ii
	LIST OF FIGURES	iv
	LIST OF TABLES	v
	LIST OF SYMBOLS	vi
1	THEORETICAL BASIS	1-1
	1.1 Introduction	1-1
	1.2 Conservation Equations	1-2
	1.2.1 Conservation Equations for Averaged Channels	1-3
	1.2.2 Conservation Equations for Lumped Channels	1-5
2	EMPIRICAL CORRELATIONS	2-1
	2.1 Fluid Properties	2-1
	2.2 Heat Transfer Coefficient Correlations	2-1
	2.3 Single-phase Friction Factor	2-2
	2.4 Two-phase Friction Factor Multiplier	2-2
	2.5 Void Fraction Correlations	2-3
	2.6 Spacer Grid Loss Coefficient	2-4
	2.7 Correlation for Turbulent Interchange	2-4
	2.8 Hetsroni Crossflow Correlation	2-7
	2.9 CE-1 Critical Heat Flux Correlation	2-7
3	NUMERICAL SOLUTION OF THE CONSERVATION EQUATIONS	3-1
	3.1 Finite Difference Equations	3-1
	3.2 Prediction-Correction Method	3-2
4	CETOP-D DESIGN MODEL	4-1
	4.1 Geometry of CETOP-D Design Model	4-1
	4.2 Application of the Transport Coefficient in the CETOP-D Model	4-2
	4.3 Description of Input Parameters	4-4
5	THERMAL MARGIN ANALYSES USING CETOP-D	5-1
	5.1 Operating Ranges	5-1
	5.2 Detailed TORC Analysis of Sample Core	5-1
	5.3 Geometry of CETOP Design Model	5-1

TABLE OF CONTENTS (cont.)

<u>Section No.</u>	<u>Title</u>	<u>Page No.</u>
	5.4 Comparison Between TORC and CETOP-D Predicted Results	5-2
	5.5 Application of Uncertainties in CETOP-D	5-2
6	CONCLUSIONS	6-1
7	REFERENCES	7-1
	Appendix A CETOP-D Version 2 User's Guide	A-1
	Appendix B Sample CETOP-D Input/Output	B-1

LIST OF FIGURES

<u>Figure No.</u>	<u>Title</u>	<u>Page No.</u>
1.1	Control Volume for Continuity Equation	1-12
1.2	Control Volume for Energy Equation	1-13
1.3	Control Volume for Axial Momentum Equation	1-14
1.4	Control Volume for Lateral Momentum Equation	1-15
3.1	CETOP-D Flow Chart	3-3
3.2	Flow Chart for Prediction-Correction Method	3-7
4.1	Channel Geometry for CETOP-D Model	4-2
5.1	Stage 1 TORC Channel Geometry for ANO-2 Cycle 2	5-3
5.2	Stage 2 TORC Channel Geometry for ANO-2 Cycle 2	5-4
5.3	Stage 3 TORC Channel Geometry for ANO-2 Cycle 2	5-5
5.4	Axial Power Distributions	5-6
5.5	Inlet Flow Distribution for ANO-2 Cycle 2, 4-Pump Operation	5-7
5.6	Exit Pressure Distribution for ANO-2 Cycle 2, 4-Pump Operation	5-8
5.7	CETOP-D Channel Geometry for ANO-2 Cycle 2	5-9

LIST OF TABLES

<u>Table No.</u>	<u>Title</u>	<u>Page No.</u>
2.1	Two-Phase Friction Factor Multiplier	2-8
2.2	Functional Relationships in the Two-Phase Friction Factor Multiplier	2-9
5.1	Comparisons Between Detailed TORC and CETOP-D	5-10

LIST OF SYMBOLS

<u>SYMBOL</u>	<u>DEFINITION</u>
A	Cross-sectional area of flow channel
CHF	Critical heat flux
d	Diameter of fuel rod
De	Hydraulic diameter
DNBR	Departure from nucleate boiling ratio
DTF	Forced convection temperature drop across coolant film adjacent to fuel rods
DTJL	Jens-Lottes nucleate boiling temperature drop across coolant film adjacent to fuel rods
f	Single phase friction factor
F	Force
f_{ϕ}, f_H, f_p	Engineering factors
\bar{F}_R	Radial power factor, equal to the ratio of local-to-average radial power
F_S	Ratio of critical heat flux for an equivalent uniform axial power distribution to critical heat flux for the actual non-uniform axial power distribution.
F_T	Total power factor, equal to the product of the local radial and axial power factors
F_z	Axial power factor, equal to the ratio of the local-to-average axial power.
g	Gravitational acceleration
G	Mass flow rate
h	Heat transfer coefficient
h	Enthalpy
K_G	Spacer grid loss coefficient
K_{ij}	Crossflow resistance coefficient
K_{∞}	Crossflow resistance coefficient
λ	Effective lateral distance over which crossflow occurs between adjoining subchannels
MDNBR	Minimum departure from nucleate boiling ratio
m	Axial flow rate
N_H, N_p, N_u	Transport coefficients for enthalpy, pressure and velocity

SYMBOLDEFINITION

P	Pressure
P_h	Heated perimeter
Pr	Prandtl Number
P_w	Wetted perimeter
q'	Heat addition per unit length
q''	Heat flux
Re	Reynolds number
s	Rod spacing or effective crossflow width
s_{REF}	Reference crossflow width
T_{cool}	Bulk coolant temperature
T_{sat}	Saturation temperature
T_{wall}	Surface temperature of fuel rod
u	Axial velocity
u^*	Effective velocity carried by diversion crossflow
v	Specific volume
V	Crossflow velocity
w_{ij}	Diversion crossflow between adjacent flow channels
w'_{ij}	Turbulent mass interchange rate between adjacent flow channels
x	Axial distance
X	Quality
α	Void fraction
γ	Slip ratio
ρ	Density
ϕ	Two-phase friction factor multiplier
ϕ_j	Heat Flux
ζ	Fraction of fuel rod being included in flow channel

SUBSCRIPTS

f, g	Liquid and vapor saturated conditions
i, j	Subchannel identification numbers
ij	Denotes hydraulic connection between subchannels i and j
J	Axial node number
P	Denotes predicted value

SUPERSCRIPTS

DEFINITION

- Denotes transported quantity between adjoining lumped channels
- * Denotes transported quantity carried by diversion crossflow
- ^ Denotes effective value

1.0 THEORETICAL BASIS

1.1 Introduction

The minimum value for the departure from nucleate boiling ratio (MDNBR) which serves as a measure for the core thermal margin, is predicted for a C-E reactor by the TORC code (Thermal-Hydraulics of a Reactor Core, Reference 1).

A multi-stage TORC modelling method (Detailed TORC), which produces a detailed three-dimensional description of the core thermal-hydraulics, requires about [] cp (central processor) seconds for each steady state calculation on the C-E CDC 7600 computer. A simplified TORC modelling method (S-TORC, Reference 5), developed to meet practical design needs, reduces the cp time to about [] seconds for each calculation on a 20-channel core representation. Such a simplification of the modelling method results in a penalty included in the S-TORC model to account for the deviation of MDNBR from that calculated by Detailed TORC. Present TORC/CE-1 methodology includes in S-TORC an adjusted hot assembly inlet flow factor to eliminate the possible nonconservatism in the MDNBR prediction produced by S-TORC.

An even simpler code, CETOP, (C-E Thermal On-Line Program, Reference 4), which utilizes the same conservation equations as those in TORC, has been used in the Core Operating Limit Supervisory System (COLSS) for monitoring MDNBR. The CETOP-D model to be described in this report has been developed to retain all capabilities the S-TORC model has in the determination of core thermal margin. It takes typically [] for CETOP-D to perform a calculation, as accurately as S-TORC, on a four-channel core representation.

For the following reasons CETOP-D is as accurate as and faster-running than its predecessor, S-TORC,: (1) it uses "transport coefficients", serving as weighting factors, for more precise treatments of crossflow and turbulent mixing between adjoining channels, and (2) it applies the "prediction-correction" method, which replaces the less efficient iteration method used in S-TORC, in the determination of coolant properties at all axial nodes.

A finalized version of a CETOP-D model includes an "adjusted" hot assembly flow factor and allows for engineering factors. The hot assembly flow factor accounts for the deviations in MDNBR due to model simplification. A statistical or deterministic allowance for engineering factors accounts for the uncertainties associated with manufacturing tolerances.

1.2 Conservation Equations

A PWR core contains a large number of subchannels which are surrounded by fuel rods or control rod guide tubes. Each subchannel is connected to its neighboring ones by crossflow and turbulent interchange through gaps between fuel rods or between fuel rods and guide tubes. For this reason, subchannels are said to be hydraulically open to each other and a PWR is said to contain an open core.

The conservation equations for mass, momentum and energy are derived in a control volume representing a flow channel of finite axial length. Two types of flow channels are considered in the representation of a reactor core: (1) averaged channels, characterized by averaged coolant conditions, and (2) lumped channels, in which boundary subchannels, contained within the main body of the channel, are used in the calculation of interactions with neighboring flow channels. An averaged channel is generally of relatively large size and is located far from the location at which MDNBR occurs. With the help of boundary subchannels, a lumped channel describes in more detail the flow conditions near the MDNBR location, and is of relatively small flow area (e.g. a local group of fuel rod subchannels).

To be more specific about the differences between the modelling schemes of the two channels, their conservation equations are separately derived.

1.2.1 Conservation Equations for Averaged Channels

1.2.1.1 Continuity Equation

Consider two adjacent channels i and j , as shown in Figure 1.1, which are hydraulically open to each other. The continuity equation for channel i has the form:

$$-m_i + \left(m_i + \frac{\partial m_i}{\partial x} dx\right) - w'_{ji} dx + w'_{ij} dx + w_{ij} dx = 0 \quad (1.1)$$

Assuming the turbulent interchanges $w'_{ij} = w'_{ji}$, the above equation becomes:

$$\frac{\partial m_i}{\partial x} = -w_{ij} \quad (1.2)$$

Considering all the flow channels adjacent to channel i , and taking w_{ij} as positive for flows from i to j , the continuity equation becomes:

$$\frac{\partial m_i}{\partial x} = - \sum_{j=1}^N w_{ij} ; i = 1, 2, 3, \dots, N \quad (1.3)$$

1.2.1.2 Energy Equation

The energy equation for channel i in Figure 1.2b, considering only one adjacent channel j , is:

$$-m_i h_i + \left(m_i h_i + \frac{\partial}{\partial x} m_i h_i dx\right) - q'_i dx - w'_{ji} h_j dx + w'_{ij} h_i dx + w_{ij} h^* dx = 0 \quad (1.4)$$

where h^* is the enthalpy carried by the diversion crossflow w_{ij} .

The above equation can be rewritten, by using Eq. (1.2) and $w'_{ij} = w'_{ji}$, as:

$$m_i \frac{\partial h_i}{\partial x} = q'_i - (h_i - h_j) w'_{ij} + (h_i - h^*) w_{ij} \quad (1.5)$$

Considering all adjacent flow channels, the energy equation becomes:

$$\frac{\partial h_i}{\partial x} = \frac{q'_i}{m_i} - \sum_{j=1}^N (h_i - h_j) \frac{w'_{ij}}{m_i} + \sum_{j=1}^N (h_i - h^*) \frac{w_{ij}}{m_i} \quad (1.6)$$

1.2.1.3 Axial Momentum Equation

Referring to Figure 1.3b, the axial momentum equation for channel i , considering only one adjacent channel j , has the form:

$$\begin{aligned} -F_i dx + p_i dA_i - gA_i \rho_i dx + p_i A_i - (p_i A_i + \frac{\partial p_i}{\partial x} A_i dx) = \\ -m_i u_i + (m_i u_i + \frac{\partial}{\partial x} m_i u_i dx) - w'_{ji} u_j dx + w'_{ij} u_i dx + w_{ij} u^* dx \end{aligned} \quad (1.7)$$

where $u^* = 1/2 (u_i + u_j)$.

By using the assumption $w'_{ij} = w'_{ji}$, one has:

$$-F_i - gA_i \rho_i - A_i \frac{\partial p_i}{\partial x} = \frac{\partial}{\partial x} m_i u_i + (u_i - u_j) w'_{ij} + u^* w_{ij} \quad (1.8)$$

Substituting the following definitions:

$$u_i \equiv \frac{m_i v p_i}{A_i}; \quad F_i \equiv \left(\frac{A_i v_i f_i \phi_i}{2De_i} + \frac{A_i K_{Gi} v_i}{2\Delta x} \right) \left(\frac{m_i}{A_i} \right)^2 \quad (1.9)$$

and Eq. (1.2) into Eq. (1.8), one obtains:

$$\begin{aligned} A_i \frac{\partial p_i}{\partial x} = -A_i \left(\frac{m_i}{A_i} \right)^2 \left[\frac{v_i f_i \phi_i}{2De_i} + \frac{K_{Gi} v_i}{2\Delta x} + A_i \frac{\partial}{\partial x} \left(\frac{v p_i}{A_i} \right) \right] - gA_i \rho_i \\ - (u_i - u_j) w'_{ij} + (2u_i - u^*) w_{ij} \end{aligned} \quad (1.10)$$

Considering all adjacent channels, the axial momentum equation becomes:

$$\frac{\partial p_i}{\partial x} = - \left(\frac{m_i}{A_i} \right)^2 \left(\frac{v_i f_i \phi_i}{2De_i} + \frac{K_{G_i} v_i}{2\Delta x} + A_i \frac{\partial}{\partial x} \left(\frac{v p_i}{A_i} \right) \right) - g \rho_i - \sum_{j=1}^N (u_i - u_j) \frac{w'_{ij}}{A_i} + \sum_{j=1}^N (2u_i - u^*) \frac{w_{ij}}{A_i} \quad (1.11)$$

1.2.1.4 Lateral Momentum Equation

For large flow channels, a simplified transverse momentum equation may be used which relates the difference in the channel-averaged pressures p_i and p_j to the crossflow w_{ij} . Referring to the control volume shown in Figure 1.4b, the form of the momentum equation is:

$$(p_i - p_j) = K_{ij} \frac{w_{ij} |w_{ij}|}{2g s^2 \rho^*} \quad (1.12)$$

where K_{ij} is a variable coefficient defined in Reference 3 as

$$K_{ij} = \left(\frac{K_{\infty}^2}{4} + XFCONS \frac{u_i^2}{v_{ij}^2} \right)^{1/2} + \frac{K_{\infty}}{2} \quad (1.13)$$

For averaged channels the spatial acceleration term is not included explicitly but is treated implicitly by means of the variable coefficient, K_{ij} .

Because the coefficients K_{∞} and XFCONS were empirically determined for rod bundles, Eq's. (1.12) and (1.13) are appropriate for channels of relatively large size.

1.2.2 Conservation Equations for Lumped Channels

1.2.2.1 Continuity Equation

Since only mass transport is considered within the control volume, the continuity equation has similar form to that for averaged channel, i.e., Eq.(1.3).

1. 2.2.2 Energy Equation

Consider two adjacent channels i and j and apply the energy conservation to channel i within the control volume as shown in Figure 1.2.a, the energy equation has the form:

$$m_i \frac{\partial h_i}{\partial x} = q'_i - (\bar{h}_i - \bar{h}_j) w'_{ij} + (h_i - h^*) w_{ij} \quad (1.14)$$

where q' = energy added to channel i from fuel rods per unit time per unit length,

w'_{ij} = turbulent interchange between channels i and j

$\bar{h}_i w'_{ij}$ = energy transferred out of channel i to j due to the turbulent interchange w'_{ij} ,

$\bar{h}_j w'_{ij}$ = energy transferred into channel i from j due to the turbulent interchange w'_{ij} ,

\bar{h}_i and \bar{h}_j are the fluid enthalpies associated with the turbulent interchange; h^* is the enthalpy carried by the diversion cross-flow w_{ij} and is determined as follows:

$$\begin{aligned} h^* &= \bar{h}_i \quad \text{if } w_{ij} \geq 0 \\ h^* &= \bar{h}_j \quad \text{if } w_{ij} < 0 \end{aligned} \quad (1.15)$$

At elevation x , the enthalpy carried by the turbulent interchange across the boundary between channels i and j is modeled as the fluid enthalpy of the boundary subchannels of the donor lumped channel. Thus, \bar{h}_i and \bar{h}_j are defined as the radially averaged enthalpies of the boundary subchannels of lumped channels i and j respectively.

Since \bar{h}_i and \bar{h}_j are not explicitly solved in the calculation, we define a transport coefficient N_H to relate these parameters to the lumped channel counterparts h_i and h_j as follows:

$$N_H = \frac{h_i - h_j}{\bar{h}_i - \bar{h}_j} \quad (1.16)$$

The parameter N_H is named the transport coefficient for enthalpy.

Using this coefficient, one can assume the coolant enthalpy at the boundary:

$$h_c = \frac{h_i + h_j}{2} = \frac{\bar{h}_i + \bar{h}_j}{2} \quad (1.17)$$

and

$$\bar{h}_i - h_c = \frac{\bar{h}_i - \bar{h}_j}{2} \quad (1.18)$$

$$\bar{h}_j - h_c = \frac{\bar{h}_j - \bar{h}_i}{2} \quad (1.19)$$

which are followed by the approximations:

$$\begin{aligned} \bar{h}_i &= h_c + (\bar{h}_i - h_c) \\ &= \frac{h_i + h_j}{2} + \frac{h_i - h_j}{2N_H}; \end{aligned} \quad (1.20)$$

$$\begin{aligned} \bar{h}_j &= h_c + (\bar{h}_j - h_c) \\ &= \frac{h_i + h_j}{2} + \frac{h_j - h_i}{2N_H} \end{aligned} \quad (1.21)$$

Inserting Eqns.(1.17)-(1.21) into Eq. 1.14, the lumped channel energy equation is derived as:

$$m_i \frac{\partial h_i}{\partial x} = q'_i - \left(\frac{h_i - h_j}{N_H} \right) w'_{ij} + \left(h_i - \left(\frac{h_i + h_j}{2} + \frac{(h_i - h_j)^n}{2N_H} \right) \right) w_{ij} \quad (1.22)$$

where $n = 1$ if $w_{ij} \geq 0$ and $n = -1$ otherwise.

It should be noted that if channels i and j were averaged channels, $N_H = 1.0$ for this case, Eq. (1.22) reduces to the Eq. (1.5) in Section 1.2.1.2.

1.2.2.3 Axial Momentum Equation

Consider two adjacent lumped channels i and j and apply the axial momentum conservation law to channel i as shown in Fig. 1.3a.

$$A_i \frac{\partial p_i}{\partial x} = -F_i - g\rho_i A_i - (\bar{u}_i - \bar{u}_j) w'_{ij} + (2u_i - u^*) w_{ij} \quad (1.23)$$

where: A_i = channel area,
 p_i = radially averaged static pressure,
 g = gravitational acceleration,
 ρ = coolant density,
 \bar{u} = axial velocity carried by the turbulent interchange
 w'_{ij}
 u = channel radially averaged velocity
 F_i = momentum force due to friction, grid form loss and density gradient, where

$$F_i = A_i \left(\frac{m_i}{A_i} \right)^2 \left[\frac{v_i f_i \phi_i}{2De_i} + \frac{K_{Gi} v_i}{2 \Delta x} + \frac{A_i \partial}{\partial x} \left(\frac{v_i p_i}{A_i} \right) \right]$$

u^* = defined as the velocity carried by diversion crossflow, $\begin{cases} u^* = \bar{u}_i & \text{if } w_{ij} \geq 0 \\ u^* = \bar{u}_j & \text{if } w_{ij} < 0 \end{cases}$

As for \bar{h}_i and \bar{h}_j , \bar{u}_i and \bar{u}_j can be regarded as the averaged velocities of the boundary subchannels of the lumped channels i and j respectively. Define the transport coefficient for axial velocity, N_U , as follows:

$$N_U = \frac{u_i - u_j}{\bar{u}_i - \bar{u}_j} \quad (1.24)$$

Using similar procedures in the approximation of \bar{h}_i and \bar{h}_j in terms of h_i , h_j , and N_H , as described from Eq. (1.17) to (1.22), we derive:

$$\bar{u}_i = \frac{u_i + u_j}{2} + \frac{u_i - u_j}{2N_U} \quad (1.25)$$

and

$$\bar{u}_j = \frac{u_i + u_j}{2} + \frac{u_j - u_i}{2N_U} \quad (1.26)$$

Inserting Eqs. (1.25) and (1.26) into Eq. (1.23), results in the axial momentum equation for lumped channels:

$$A_i \frac{\partial p_i}{\partial x} = -F_i - A_i g \rho_i - \left(\frac{u_i - u_j}{N_U} \right) w'_{ij} + \left(2u_i - \left(\frac{u_i + u_j}{2} + \frac{(u_i - u_j)n}{2N_U} \right) \right) w_{ij} \quad (1.27)$$

where n is defined in Eq. (1.22)

1.2.2.4 Lateral Momentum Equation

Consider the rectangular control volume in the gap region between channels i and j as shown in Figure 1.4.a. Assuming that the difference between the diversion crossflow momentum fluxes entering and leaving the control volume through the vertical surfaces $s\Delta x$ is negligibly small, the formulation for lateral momentum balance is:

$$-F_{ij} - \bar{p}_j s\Delta x + \bar{p}_i s\Delta x = -(\rho^* s \ell u^* V)_x + (\rho^* s \ell u^* V)_{x+\Delta x} \quad (1.28)$$

Making use of the definition of the lateral flow rate

$$w_{ij} = \rho^* sV$$

Eq. (1.28) becomes, after rearranging:

$$(\bar{p}_i - \bar{p}_j) = \frac{F_{ij}}{s\Delta x} + \frac{1}{s/\ell} \frac{\Delta(u^* w_{ij})}{\Delta x} \quad (1.29)$$

The term $F_{ij}/s\Delta x$ represents the lateral shear stress acting on the control volume due to crossflow and is defined as:

$$\frac{F_{ij}}{s\Delta x} = K_{ij} \frac{w_{ij} |w_{ij}|}{2g s^2 \rho^*} \quad (1.30)$$

Substituting Eq. (1.30) into Eq. (1.29), and taking the limit as $\Delta x \rightarrow 0$,

$$(\bar{p}_i - \bar{p}_j) = K_{ij} \frac{w_{ij} |w_{ij}|}{2g s^2 \rho^*} + \frac{1}{s/\ell} \frac{\partial}{\partial x} (u^* w_{ij}) \quad (1.31)$$

where: \bar{p} = channel averaged pressure,

K_{ij} = cross-flow resistance coefficient,

w_{ij} = diversion cross-flow between channels i and j,

s = gap width between fuel rods,

ℓ = effective length of transverse momentum interchange,

u^* = axial velocity carried by the diversion cross-flow w_{ij} ,
assumed to be $(u_i + u_j)/2$

ρ^* = density of the diversion crossflow where $\begin{cases} \rho^* = \rho_i; w_{ij} \geq 0 \\ \rho^* = \rho_j; w_{ij} < 0 \end{cases}$

The above equation is equally well applied to two lumped channels when each contains a certain number of subchannels arranged as shown in Figure 1.4a. In this case, the diversion cross-flow w_{ij} and the gap width s should be expressed by:

$$w_{ij} = (N) \text{ (cross-flow through gap between two adjacent rods)} \quad (1.32)$$

$$s = (N) \text{ (gap between two adjacent rods)} \quad (1.33)$$

where N is the number of the boundary subchannels contained in each of the lumped channels. For the case of two generalized three-dimensional lumped channels, parameters \bar{p}_i and \bar{p}_j are regarded as the radially averaged static pressures of the boundary subchannels of the lumped channels i and j respectively. As shown in Fig. 1.4a., the transverse momentum between two generalized lumped channels are governed by the following equation:

$$\bar{p}_i - \bar{p}_j = K_{ij} \frac{w_{ij}|w_{ij}|}{2gs^2\rho^*} + \frac{\ell}{s} \frac{\partial(u^*w_{ij})}{\partial x} \quad (1.34)$$

It should be noted that the transverse momentum equation for the generalized lumped channels i and j in Fig. 1.4a is the same as that for the boundary subchannels. This is because the control volumes chosen to model the transverse momentum transport in these two cases are identical. Since \bar{p}_i and \bar{p}_j are not explicitly calculated, we define the transport coefficient for pressure to relate these parameters to the calculated lumped channel parameters p_i and p_j as follows:

$$N_p = \frac{p_i - p_j}{\bar{p}_i - \bar{p}_j} \quad (1.35)$$

where p_i and p_j are the radially averaged static pressures of the lumped channels i and j respectively. Inserting Eq. (1.35) into Eq. (1.34), we obtain the transverse momentum equation for three-dimensional lumped channels as follows:

$$\frac{p_i - p_j}{N_p} = K_{ij} \frac{w_{ij}|w_{ij}|}{2gs^2\rho^*} + \frac{\ell}{s} \frac{\partial(u^*w_{ij})}{\partial x} \quad (1.36)$$

1.2.2.5 Transport Coefficients

There are three transport coefficients N_H , N_U and N_p in Eqs. (1.16), (1.24) and (1.35) which need to be evaluated prior to the calculation of conservation equations. Previous study in Reference 2 concluded that the calculated h_i , m_i , p_i , and w_{ij} are insensitive to the values used for N_U and N_p . This conclusion is further confirmed for the three-dimensional lumped channels. Therefore, the values of N_U and N_p can be estimated by a detailed subchannel analysis and used for a given reactor core under all possible operating conditions. It is, however, not the case for N_H , whose value is strongly dependent upon radial power distribution and also a function of axial power shape, core average heat flux, channel axial elevation, coolant inlet temperature, system pressure, and inlet mass velocity.

A value of N_H can be calculated by using a detailed subchannel TORC analysis to determine h_i , h_j , \bar{h}_i , \bar{h}_j and N_H for use in the CETOP-D lumped channel analysis. However an alternate method is used in CETOP-D, utilizing the power distribution and the basic operating parameters input into CETOP-D to determine N_H for each axial finite-difference node. [

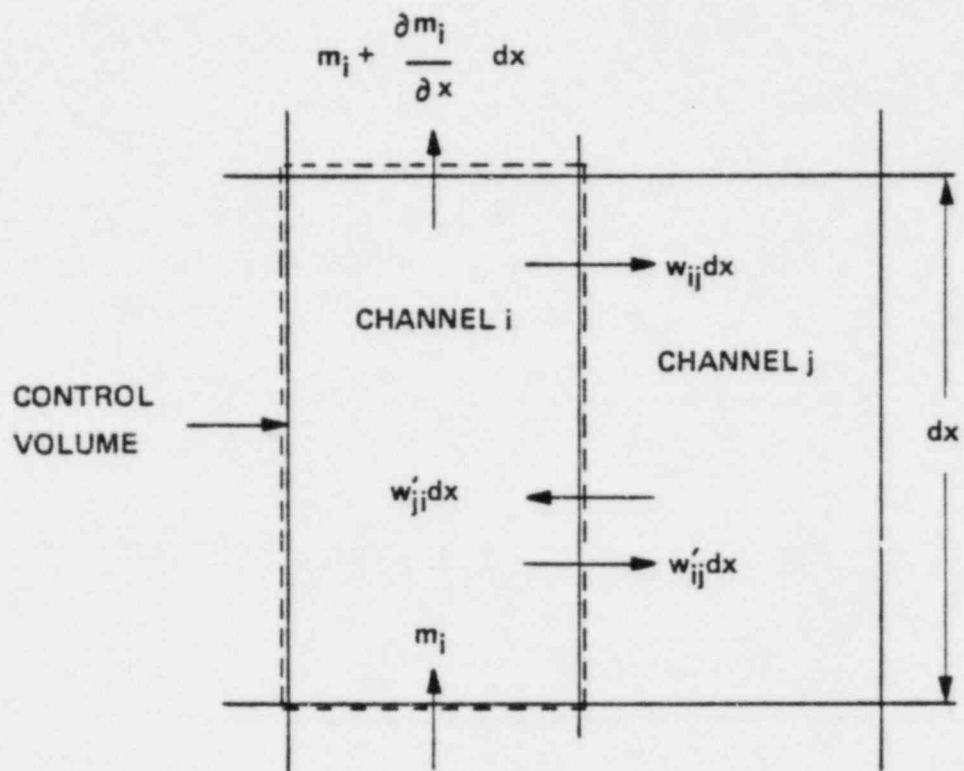
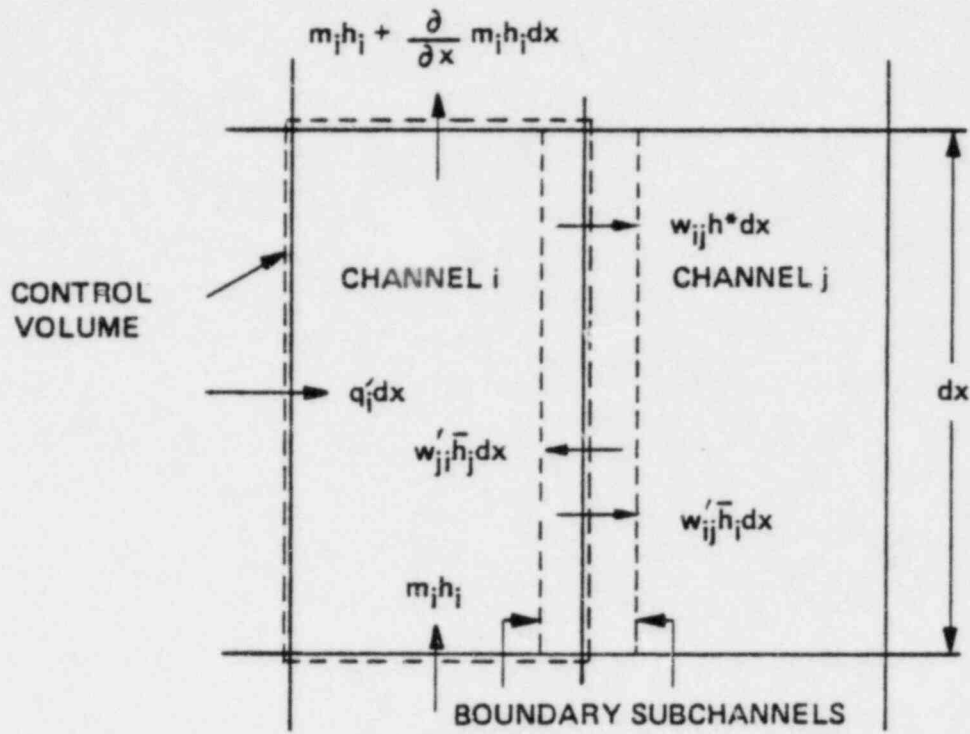
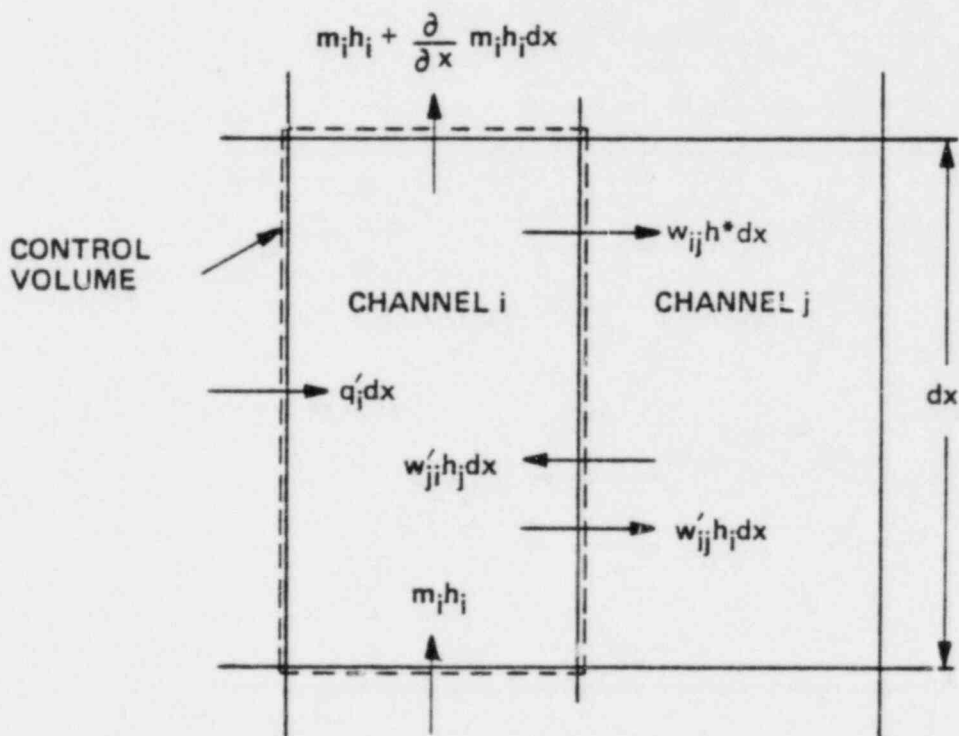


Figure 1.1
CONTROL VOLUME FOR CONTINUITY EQUATION

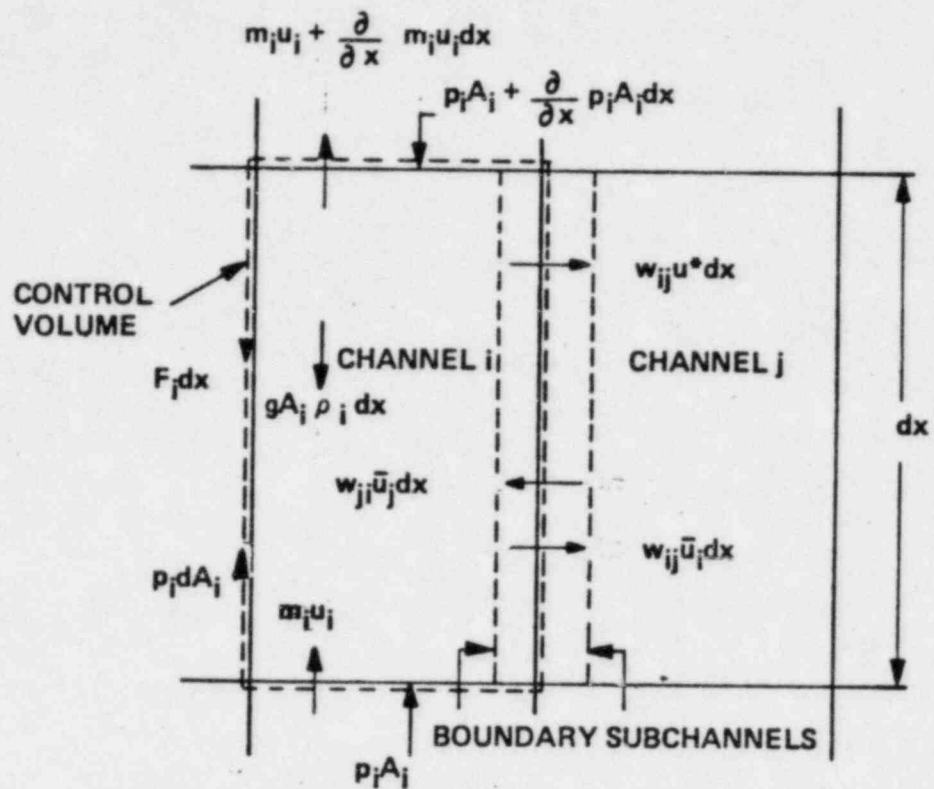


(A) CONTROL VOLUME FOR LUMPED CHANNEL

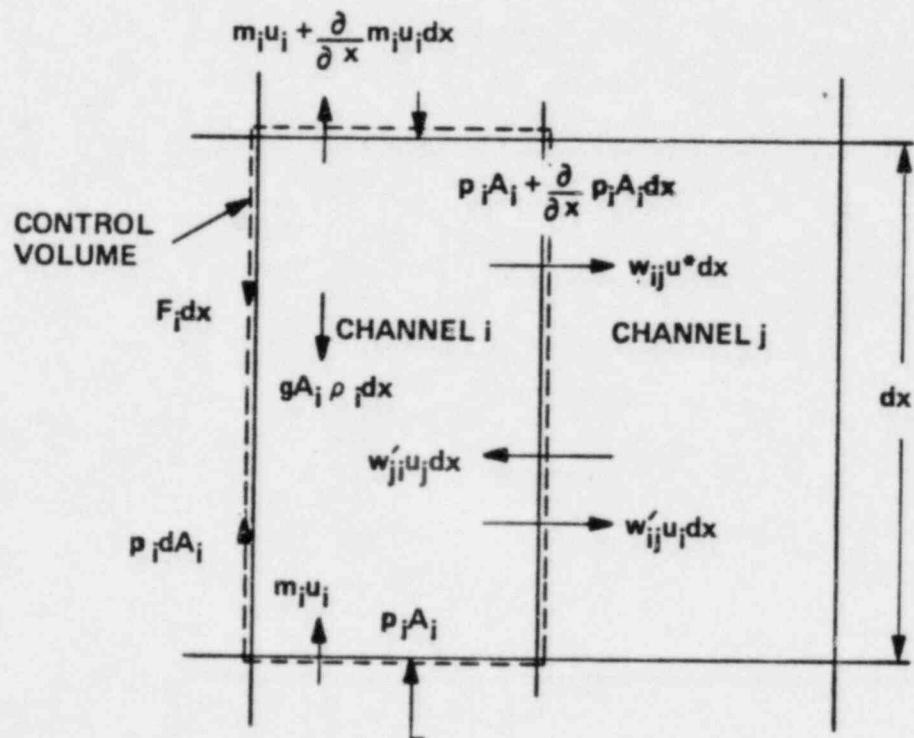


(B) CONTROL VOLUME FOR AVERAGED CHANNEL

Figure 1.2
CONTROL VOLUMES FOR ENERGY EQUATION

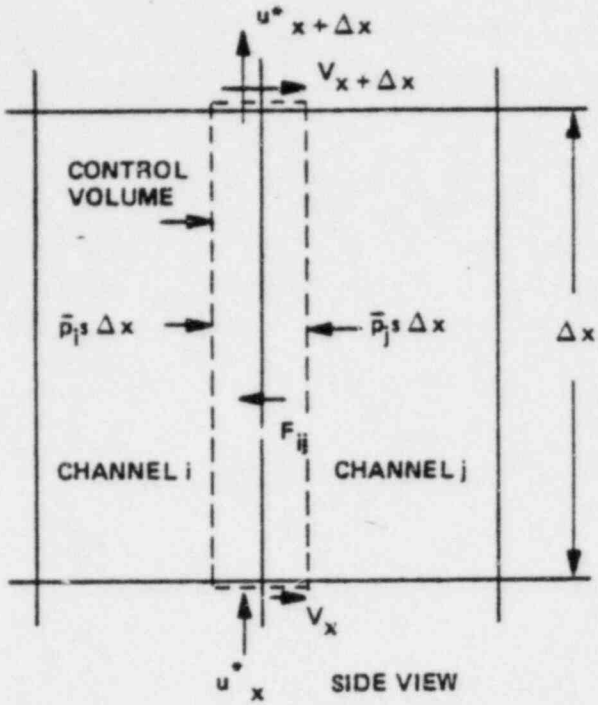


(A) CONTROL VOLUME FOR LUMPED CHANNEL

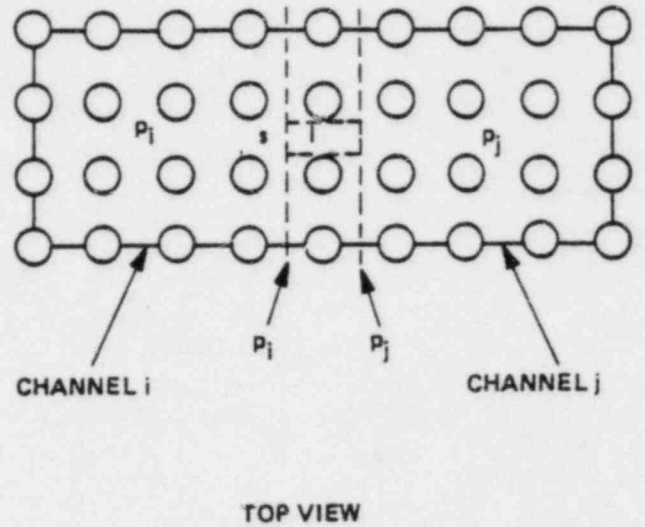


(B) CONTROL VOLUME FOR AVERAGED CHANNEL

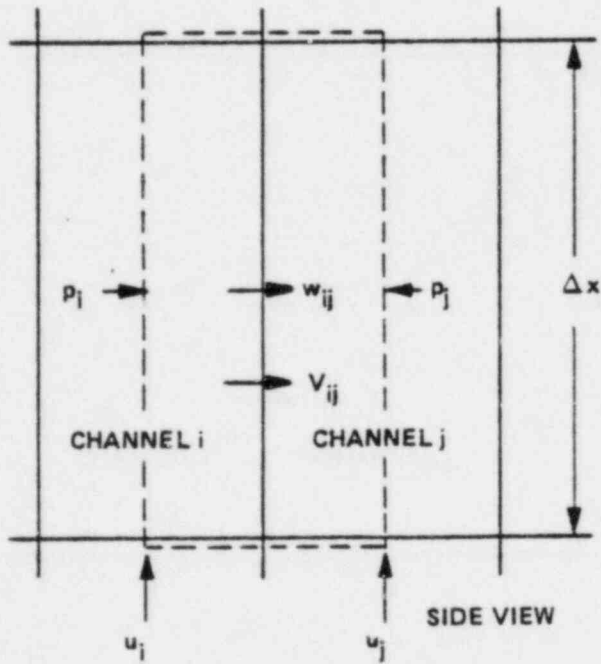
Figure 1.3
CONTROL VOLUMES FOR AXIAL MOMENTUM EQUATION



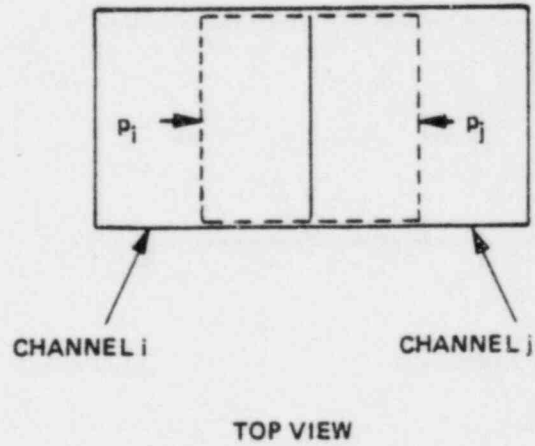
(A) CONTROL VOLUME FOR LUMPED CHANNEL



TOP VIEW



(B) CONTROL VOLUME FOR AVERAGED CHANNEL



TOP VIEW

Figure 1.4
CONTROL VOLUMES FOR LATERAL MOMENTUM EQUATION
1-15

2.0 EMPIRICAL CORRELATIONS

CETOP-D retains the empirical correlations which fit current C-E reactors and the ASME steam table routines which are included in the TORC code.

In CETOP-D, the following correlations are used:

2.1 Fluid Properties

Fluid properties are determined with a series of subroutines that use a set of curve-fitted equations developed in References 7 and 8 for describing the fluid properties in the ASME steam tables. In CETOP-D, these equations cover the subcooled and saturated regimes.

2.2 Heat Transfer Coefficient Correlations

The film temperature drop across the thermal boundary layer adjacent to the surface of the fuel cladding is dependent on the local heat flux, the temperature of the local coolant, and the effective surface heat transfer coefficient:

$$DTF = T_{\text{wall}} - T_{\text{cool}} = \frac{q''}{h} \quad (2.1)$$

For the forced convection, non-boiling regime, the surface heat transfer coefficient h is given by the Dittus-Boelter correlation, Reference 9:

$$h = \frac{0.023}{De} k(Re)^{0.8} (Pr)^{0.4} \quad (2.2)$$

For the nucleate boiling regime, the film temperature drop is determined from the Jens-Lottes correlation, Reference 10:

$$DTJL = (T_{\text{sat}} - T_{\text{cool}}) + \frac{60 (q''/10^6)^{0.25}}{P/900} \quad (2.3)$$

The initiation of nucleate boiling is determined by calculating the film temperature drop on the bases of forced convection and nucleate boiling.

$$DTJL < DTF,$$

nucleate boiling is said to occur.

2.3 Single-Phase Friction Factor

The single-phase friction factor, f , used for determining the pressure drop due to shear drag on the bare fuel rods under single-phase conditions is given by the Blasius form:

$$f = AA + BB (Re)^{CC} \quad (2.4)$$

2.4 Two-Phase Friction Factor Multiplier

A friction factor multiplier, ϕ , is applied to the single-phase friction factor, f , to account for two-phase effects:

$$\text{Total Friction Factor} = \phi f. \quad (2.5)$$

CETOP-D considers Sher-Green and Modified Martinelli-Nelson correlations as listed in Tables 2.1 and 2.2.

For isothermal and non-boiling conditions, the friction factor multiplier ϕ is set equal to 1.0.

For local boiling conditions, correlations by Sher and Green (Reference 11) are used for determining ϕ . The Sher-Green correlation for friction factor multiplier also accounts implicitly for the change in pressure drop due to subcooled void effects. When this correlation is used, it is not necessary to calculate the subcooled void fraction explicitly.

For bulk boiling conditions, ϕ is determined from Martinelli-Nelson results of Reference 12 with modifications by Sher-Green (Reference 11) and by

Pyle (Reference 13) to account for mass velocity and pressure level dependencies.

2.5 - Void Fraction Correlations

The modified Martinelli-Nelson correlation is used for calculating void fraction in the following ways:

- 1) For pressures below 1850 psia, the void fraction is given by the Martinelli-Nelson model from Reference 12:

$$\alpha = B_0 + B_1 X + B_2 X^2 + B_3 X^3 \quad (2.6)$$

where the coefficients B_n are defined in Reference 10 as follows:

For the quality range $0 \leq X < 0.01$:

$B_0 = B_1 = B_2 = B_3 = 0$; the homogeneous model is used for calculating void fraction:

$$\begin{aligned} \alpha &= 0 && \text{For } X \leq 0 \\ \alpha &= \frac{X v_g}{(1-X)v_f + Xv_g} && \text{For } X > 0 \end{aligned} \quad (2.7)$$

For the quality range $0.01 \leq X \leq 0.10$:

$$\begin{aligned} B_0 &= 0.5973 - 1.275 \times 10^{-3} p + 9.019 \times 10^{-7} p^2 - 2.065 \times 10^{-10} p^3 \\ B_1 &= 4.746 + 4.156 \times 10^{-2} p - 4.011 \times 10^{-5} p^2 + 9.867 \times 10^{-9} p^3 \\ B_2 &= -31.27 - 0.5599 p + 5.580 \times 10^{-4} p^2 - 1.378 \times 10^{-7} p^3 \\ B_3 &= 89.07 + 2.408 p - 2.367 \times 10^{-3} p^2 + 5.694 \times 10^{-7} p^3 \end{aligned} \quad (2.8)$$

For the quality range $0.10 < X$

$$\begin{aligned} B_0 &= 0.7847 - 3.900 \times 10^{-4} p + 1.145 \times 10^{-7} p^2 - 2.711 \times 10^{-11} p^3 \\ B_1 &= 0.7707 + 9.619 \times 10^{-4} p - 2.010 \times 10^{-7} p^2 + 2.012 \times 10^{-11} p^3 \\ B_2 &= -1.060 - 1.194 \times 10^{-3} p + 2.618 \times 10^{-7} p^2 - 6.893 \times 10^{-12} p^3 \end{aligned} \quad (2.9)$$

$$B_3 = 0.5157 + 6.506 \times 10^{-4} p - 1.938 \times 10^{-7} p^2 + 1.925 \times 10^{-11} p^3$$

- 2) At pressures equal to or greater than 1850 psia, the void fraction is given by the homogeneous flow relationship (slip ratio = 1.0):

$$\alpha = \frac{X v_g}{(1-X)v_f + X v_g}, \text{ for } p \geq 1850 \text{ psia} \quad (2.10)$$

2.6 Spacer Grid Loss Coefficient

The loss coefficient correlation for representing the hydraulic resistance of the fuel assembly spacer grids has the form:

$$K_G = D_1 + D_2 (Re)^{D_3} \quad (2.11)$$

Appropriate values for D_n must be specified for the particular grids in the problem.

2.7 Correlation for Turbulent Interchange

Turbulent interchange, which refers to the turbulent eddies caused by spacer grids, is calculated at channel boundary in the following correlation:

$$w'_{ij} = \bar{G} D_e \left(\frac{s}{s_{REF}} \right)^A (Re)^B \quad (2.12)$$

where: \bar{G} = channel averaged mass flow rate
 \bar{D}_e = channel averaged hydraulic diameter
 s = actual gap width for turbulent interchange
 s_{REF} = reference gap width defined as total gap width for one side of a complete fuel bundle divided by the number of subchannels along this side

Constants A and B are chosen as 0.0035 and 0 respectively in the present version of CETOP-D.

2.8 Hetsroni Cross Flow Correlation

Berringer, et al, proposed in Reference 15 a form of the lateral momentum equation that uses a variable coefficient for relating the static pressure difference and lateral flow between two adjoining open flow channels.

$$(\dot{p}_i - p_j) = \frac{K_{ij} w_{ij} |w_{ij}|}{2g\rho^* s^2} \quad (2.13)$$

In Berringer's treatment, the variable K_{ij} accounts for the large inertial effects encountered when the predominately axial flow is diverted in the lateral direction. In Reference 3, Hetsroni expanded the definition of K_{ij} to include the effects of shear drag and contraction-expansion losses on the lateral pressure difference:

$$K_{ij} = \frac{K_{\infty}}{2} + \left(\frac{K_{\infty}^2}{4} + (XFCONS) \frac{u_i^2}{V_{ij}^2} \right)^{1/2} \quad (2.14)$$

The terms in Eq. (2.14) involving K_{∞} represent the lateral pressure losses due to shear drag and the contraction-expansions of the flow in the absence of axial flow, i.e., lateral flow only. The third term on the right hand side of Eq. (2.14) represents the lateral pressure difference developed by the centrifugal forces as the axially directed flow is diverted laterally. This term accounts implicitly for the flow inertia effects that are treated explicitly in Eq. (1.31) by means of the momentum flux term.

Hetsroni suggested $K_{\infty} = 1.4$ and $XFCONS = 4.2$ for rod bundle fuel assemblies. These values are also used in CETOP-D.

2.9 CE-1 Critical Heat Flux (CHF) Correlation (Reference 14)

The CE-1 CHF correlation included in the CETOP-D is of the following form:

$$\frac{q''_{CHF}}{10^6} = \frac{b_1 \left(\frac{d}{d_m}\right)^{b_2} \left((b_3 + b_4 P) \left(\frac{G}{10^6}\right)^{(b_5 + b_6 P)} - \left(\frac{G}{10^6}\right) (x) (h_{fg}) \right)}{\left(\frac{G}{10^6}\right) (b_7 P + b_8 G/10^6)}$$

where: q''_{CHF} = critical heat flux, BTU/hr-ft²
 p = pressure, psia
 d = heated equivalent diameter of the subchannel, inches
 d_m = heated equivalent diameter of a matrix subchannel with the same rod diameter and pitch, inches
 G = local mass velocity at CHF location, lb/hr-ft²
 x = local coolant quality at CHF location, decimal fraction
 h_{fg} = latent heat of vaporization, BTU/lb

and $b_1 = 2.8922 \times 10^{-3}$
 $b_2 = -0.50749$
 $b_3 = 405.32$
 $b_4 = -9.9290 \times 10^{-2}$
 $b_5 = -0.67757$
 $b_6 = 6.8235 \times 10^{-4}$
 $b_7 = 3.1240 \times 10^{-4}$
 $b_8 = -8.3245 \times 10^{-2}$

The above parameters were defined from source data obtained under following conditions:

pressure (psia)	1785 to 2415
local coolant quality	-0.16 to 0.20
local mass velocity (lb/hr-ft ²)	0.87×10^6 to 3.2×10^6
inlet temperature (°F)	382 to 644
subchannel wetted equivalent diameter (inches)	0.3588 to 0.5447
subchannel heated equivalent diameter (inches)	0.4713 to 0.7837
heated length (inches)	84,150

To account for a non-uniform axial heat flux distribution, a correction factor FS is used. The FS factor is defined as:

$$FS = \frac{q''_{CHF, \text{ Equivalent Uniform}}}{q''_{CHF, \text{ Non-uniform}}}$$

$$FS(J) = \frac{C(J)}{q''(J) (1 - e^{-C(J)x(J)})} \int_0^{x(J)} q''(x) e^{-C(J)(x(J)-x)} dx$$

where, for CE-1 CHF correlation,

$$C(J) = 1.8 \frac{(1-x_{CHF})^{4.31}}{(G/10^6)^{0.478}} \text{ ft}^{-1}$$

The departure from nucleate boiling ratio, DNBR, is:

$$\text{DNBR}(J) = \frac{1}{\text{FS}(J)} \frac{q''_{\text{CHF, Equivalent Uniform}}}{q''(J)}$$

TABLE 2.1
TWO-PHASE FRICTION FACTOR MULTIPLIER

8-2 PRESSURE, P - PSIA	3206	$\phi = 1.0$ OR $f_1(P, G, \theta^\circ/DTF)$, WHICHEVER IS LARGER	$G > 0.7 \times 10^6$ $\phi = FAM(X, G, P = 2000)$ $\times \frac{FMN_3(X, P)}{FMN_3(X, P = 2000)}$	$\phi = FAM(X, G, P = 2000) \times \frac{FMN_3(X, P)}{FMN_3(X, P = 2000)}$	$\phi = FAM(X = 0.4, G, P = 2000)$ $\times \frac{FMN_3(X, P = 2000)}{FMN_3(X = 0.4, P = 2000)}$ $\times \frac{FMN_3(X, P)}{FMN_3(X, P = 2000)}$
	2000		$G < 0.7 \times 10^6$ $\phi = FAM(X, G = 0.7, P = 2000)$ $\times \frac{FMN_3(X, P)}{FMN_3(X, P = 2000)} \times f_4(G)$	$\phi = FAM(X, G = 0.7, P = 2000) \times \frac{FMN_3(X, P)}{FMN_3(X, P = 2000)} \times f_4(G)$	$\phi = FAM(X = 0.4, G = 0.7, P = 2000)$ $\times \frac{FMN_3(X, P = 2000)}{FMN_3(X = 0.4, P = 2000)}$ $\times \frac{FMN_3(X, P)}{FMN_3(X, P = 2000)} \times f_4(G)$
	2000	$\phi = 1.0$ OR $f_1(P, G, \theta^\circ/DTF)$, WHICHEVER IS LARGER	$G > 0.7 \times 10^6$ $\phi = FAM(X, G, P = 2000)$ $\times \frac{FMN_1(X, P)}{FMN_1(X, P = 2000)}$	$\phi = FAM(X, G, P = 2000)$ $\times \frac{FMN_2(X, P)}{FMN_2(X, P = 2000)}$	$\phi = FAM(X = 0.4, G, P = 2000)$ $\times \frac{FMN_2(X, P = 2000)}{FMN_2(X = 0.4, P = 2000)}$ $\times \frac{FMN_2(X, P)}{FMN_2(X, P = 2000)}$
	1850		$G < 0.7 \times 10^6$ $\phi = FAM(X, G = 0.7, P = 2000)$ $\times \frac{FMN_1(X, P)}{FMN_1(X, P = 2000)} \times f_4(G)$	$\phi = FAM(X, G = 0.7, P = 2000)$ $\times \frac{FMN_2(X, P)}{FMN_2(X, P = 2000)} \times f_4(G)$	$\phi = FAM(X = 0.4, G = 0.7, P = 2000)$ $\times \frac{FMN_2(X, P = 2000)}{FMN_2(X = 0.4, P = 2000)}$ $\times \frac{FMN_2(X, P)}{FMN_2(X, P = 2000)} \times f_4(G)$
	1850	$\phi = 1.0$ $\times \left[\frac{T - DTJL}{T_{sat} - DTJL} \right]$ $\times \left[\frac{FMN_1(X = 0.042, P) \cdot 1}{1} \right]$	$G > 0.7 \times 10^6$ $\phi = f_2(P, G)$	$\phi = FMN_1(X, P)$ $\times f_2(P, G)$	$\phi = FMN_2(X, P) \times f_2(P, G)$
	14.7		$G < 0.7 \times 10^6$ $\phi = f_3(P, G)$	$\phi = FMN_1(X, P)$ $\times f_3(P, G)$	$\phi = FMN_2(X, P) \times f_3(P, G)$
	HEATING NO BOILING	LOCAL BOILING	BULK BOILING		
	0	0	0.02	0.2	0.4
			QUALITY, X		
			1.0		

NOTE: FUNCTIONAL RELATIONSHIPS ARE LISTED IN TABLE 2.2

Table 2.2

Functional Relationships in
the Two-Phase Friction
Factor Multiplier
(References 11,12,13)

For local boiling:

$$f_1 = C_1 \left(1 + 0.76 \left(\frac{3500-P}{1500} \right) \left(\frac{10^6}{G} \right)^{2/3} \omega \right)$$

where $C_1 = (1.05) (1 - 0.0025e^*)$

e^* = The smaller of DTJL and DTF

$$\omega = 1 - e^*/DTF$$

For bulk boiling:

$$FAM = 1 + \frac{7X^{0.75}}{(G/10^6)^{1+X}}$$

$$FMN1 = \frac{X(0.9326 - (0.2263 \times 10^{-3})P)}{1.65 \times 10^{-3} + (2.988 \times 10^{-5})P - (2.528 \times 10^{-9})P^2 + (1.14 \times 10^{-11})P^3}$$

$$FMN2 = \frac{X(1.0205 - (0.2053 \times 10^{-3})P)}{7.876 \times 10^{-4} + (3.177 \times 10^{-5})P - (8.728 \times 10^{-9})P^2 + (1.073 \times 10^{-11})P^3}$$

$$FMN3 = 1 + (-0.0103166X + 0.005333X^2) (P - 3206)$$

$$F_2 = 1.26 - 0.0004 P + 0.119 \left(\frac{10^6}{G} \right) + 0.00028 P \left(\frac{10^6}{G} \right)$$

$$f_3 = 1.36 + 0.0005 P + 0.1 \left(\frac{G}{10^6} \right) - 0.000714 P \left(\frac{G}{10^6} \right)$$

$$f_4 = 1 + 0.93 \left(0.7 - \frac{G}{10^6} \right)$$

3. NUMERICAL SOLUTION OF THE CONSERVATION EQUATIONS

3.1 Finite Difference Equations

The CETOP-D code solves the conservation equations described in Section 1 by the finite difference method. The flow chart shown in Figure 3.1 displays briefly the marching CETOP-D follows in order to search for the minimum value and the location of DNBR in a 4-channel core representation (c.f. Section 4.1).

Equations (1.2), (1.22), (1.27) and (1.36) which govern the mass, energy and momentum transport within channel i of finite axial length Δx are written in the following finite difference forms:

(1) Continuity Equation

$$\frac{m_i(J) - m_i(J-1)}{\Delta x} = -w_{ij}(J) \quad (3.1)$$

(2) Energy Equation

$$m_i(J-1) \frac{h_i(J) - h_i(J-1)}{\Delta x} = q_i' - \left\{ \frac{h_i - h_j}{N_H} w_{ij}' \right. \\ \left. - h_i w_{ij} + \left(\frac{h_i + h_j}{2} + \frac{(h_i - h_j)n}{2N_H} \right) w_{ij} \right\} \quad J-1 \quad (3.2)$$

(3) Axial Momentum Equation

$$A_i \frac{p_i(J) - p_i(J-1)}{\Delta x} = -F_i - A_i g_{p_i}(J) - \left\{ \frac{u_i - u_j}{N_U} w_{ij}' \right\}$$

$$- 2u_i w_{ij} + \left(\frac{u_i + u_j}{2} + \frac{(u_i - u_j)n}{2N_U} \right) w_{ij} \Bigg\}_J \quad (3.3)$$

(4) Lateral Momentum Equation

$$\frac{p_i(J-1) - p_j(J-1)}{N_p} = K_{ij} \frac{w_{ij}(J) w_{ij}(J)}{2g_s^2 \rho^*} + \frac{\rho}{s} \frac{u^*(J) w_{ij}(J) - u^*(J-1) w_{ij}(J-1)}{\Delta x} \quad (3.4)$$

Where J is the axial elevation indicator and Δx is the axial nodal length.

3.2 Prediction - Correction Method

In CETOP-D a non-iterative numerical scheme is used to solve the conservation equations. This prediction-correction method provides a fast yet accurate scheme for the solution of m_i , h_i , w_{ij} and p_i at each axial level. The steps used in the CETOP-D solution are as follows:

The channel flows, m_i , enthalpies h_i , pressures p_i and fluid properties are calculated at the node interfaces. The linear heat rates q_i' , cross-flows, w_{ij} , and turbulent mixing, w_{ij} , are calculated at mid-node. The solution method starts at the bottom of the core and marches upward using the core inlet flows as one boundary condition and equal core exit pressures as another.

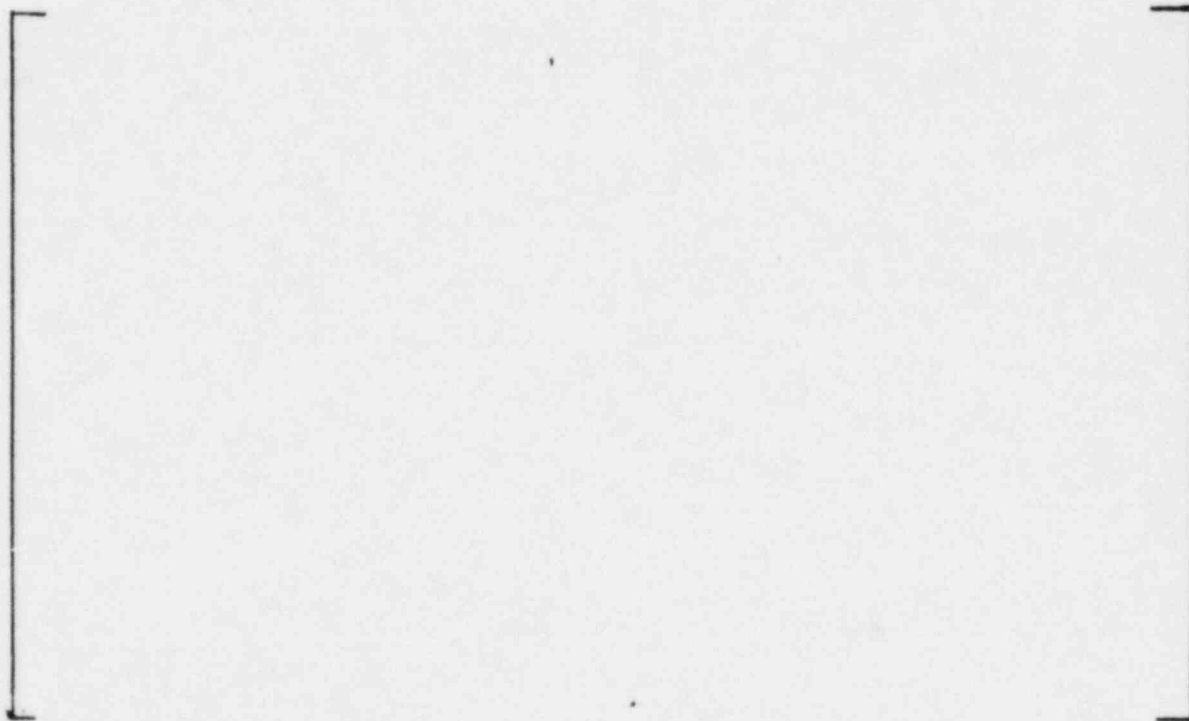
An initial estimate is made of the subchannel crossflows for nodes 1 and 2. These crossflows are set to zero.

$$w_{ij}(1) = w_{ij}(2) = 0$$

The channel flows and enthalpies at node 1 are known to be the inlet conditions. Using these initial conditions the marching technique proceeds to calculate the enthalpies and flows from node 2 to the exit node.

In this discussion "J" will designate the axial level "i" and "j" are used to designate channels.

Step



The success of this non-iterative, prediction-correction method lies in the fact that the lateral pressure difference, $p_1(J) - p_2(J)$, using the "guessed" diversion crossflow, $w_{ij}(J + 1)_p$, is a good approximation. Thus at each node the axial flow rate can be accurately determined.

TORC on the other hand, initially assumes $p_i - p_j = 0$ at each axial location. The conservation of mass and momentum equations are used to evaluate the diversion crossflows and, in turn, the flow rates at all locations. The axial momentum equation is used to determine $p_i - p_j$ for the next iteration. The iteration stops when the change in the axial flow at each location is less than a specified tolerance. Even though the prediction-correction method is a once-through marching technique, its results are very close to those from the TORC iterative numerical technique. In general, about [] in TORC to achieve the same accuracy as the prediction-correction method. In the TORC iteration scheme the transverse pressures and the flows are only updated after the iteration is completed. Therefore in marching up the core errors in the transverse pressures cause the errors in the flows and enthalpies to accumulate up the core. In the prediction-correction scheme the transverse pressures and the axial flows are corrected at each node before the next is calculated. Therefore the accumulated errors are greatly reduced. It is the accumulated errors in the downstream nodes which often force the TORC method to continue to iterate.

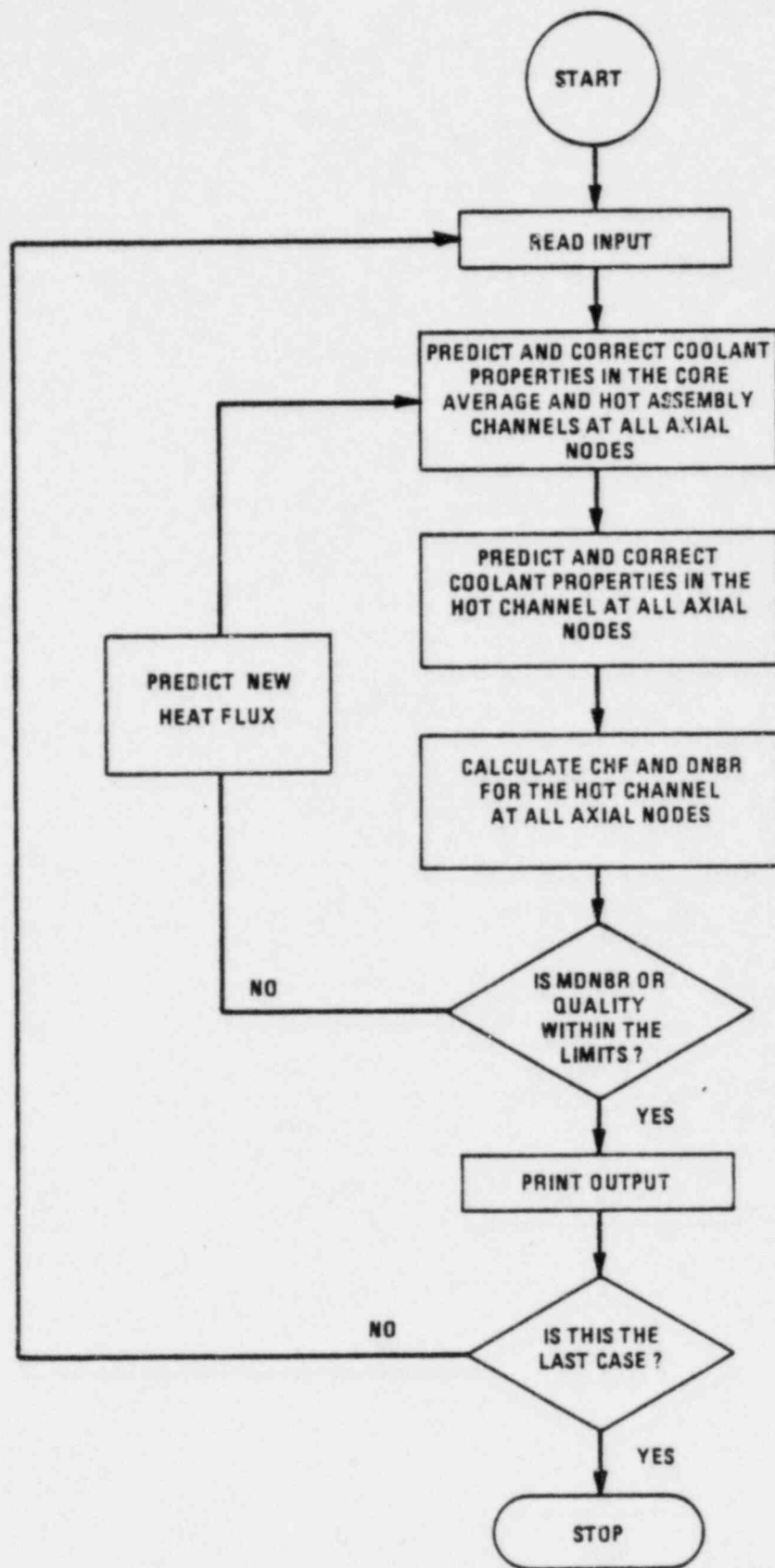


Figure 3.1
CETOP-D FLOW CHART

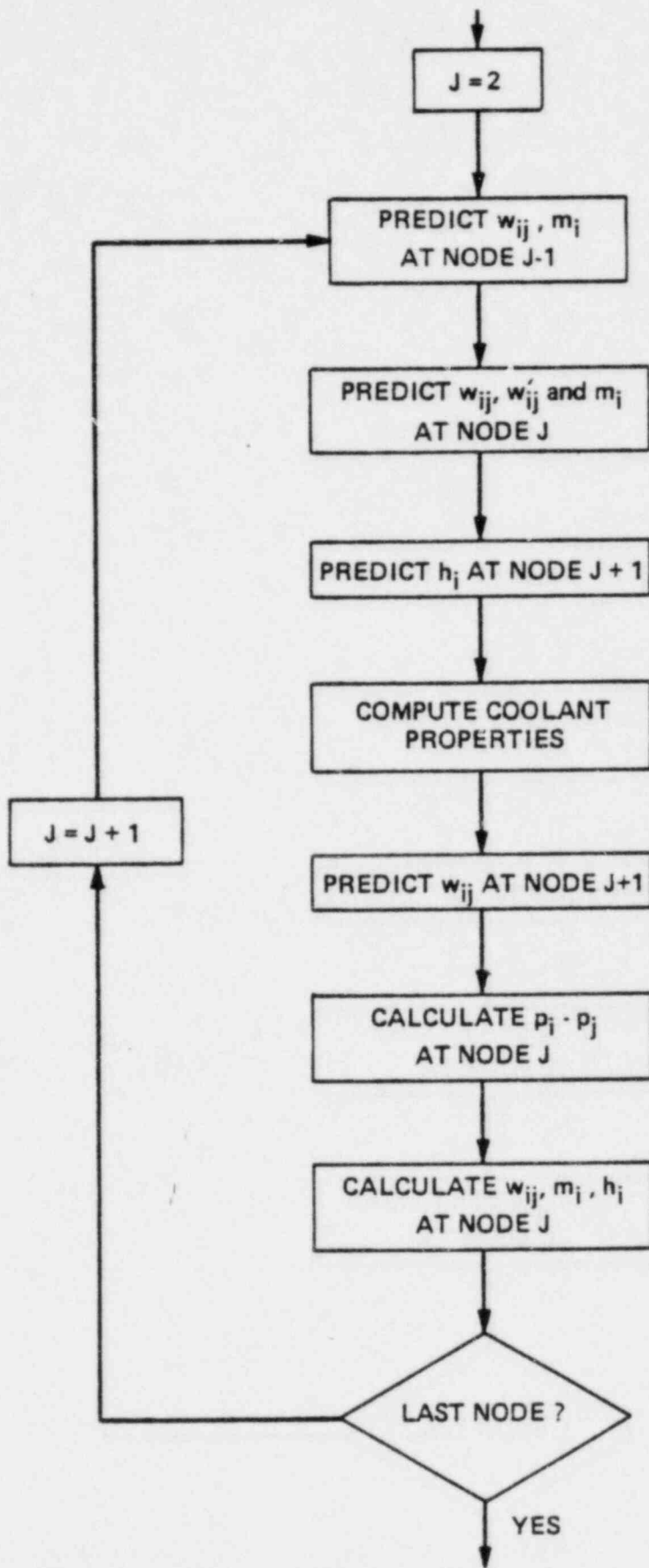


Figure 3.2

FLOW CHART FOR PREDICTION - CORRECTION METHOD

4. CETOP-D DESIGN MODEL

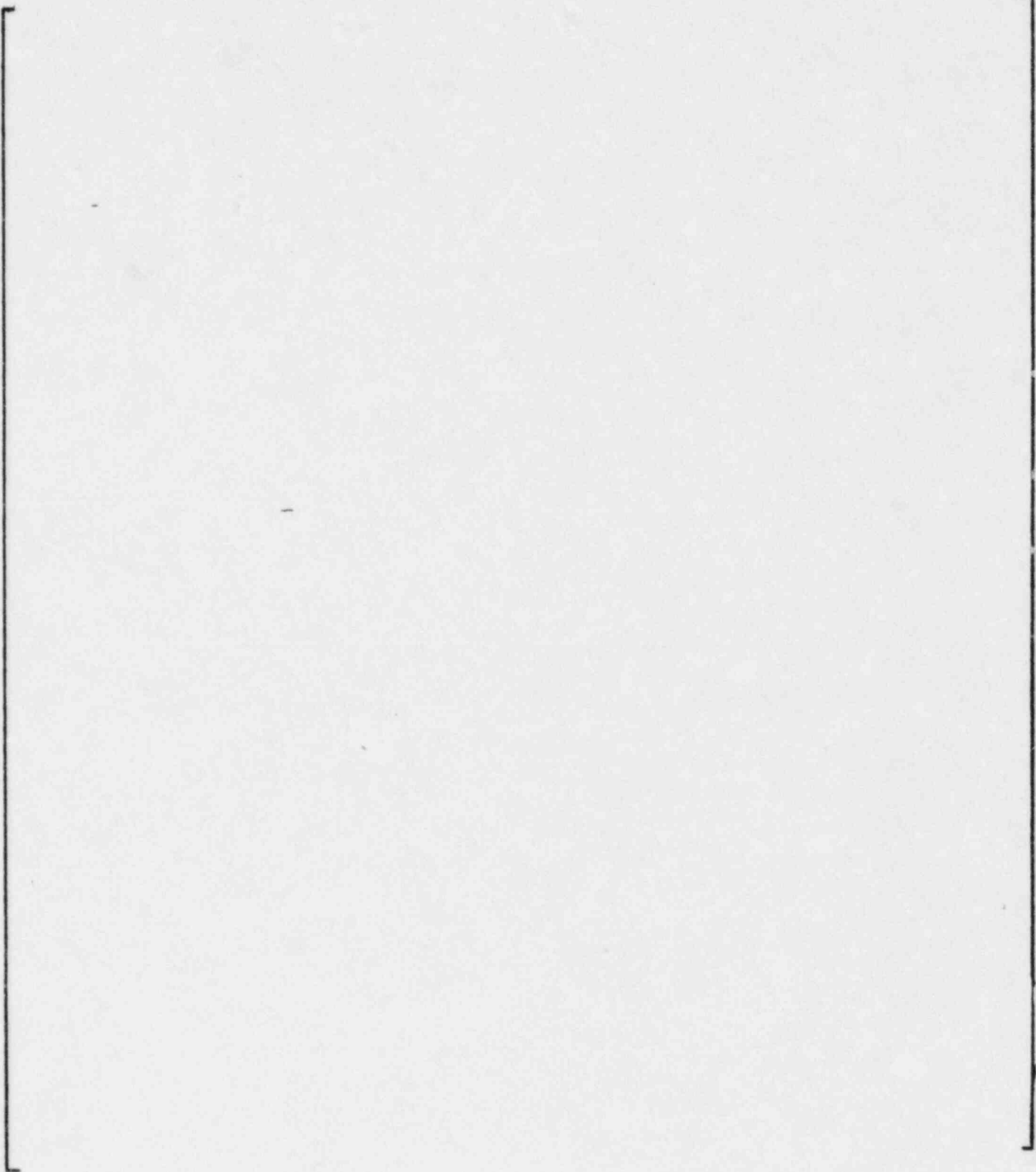
The CETOP-D code has been developed, using the basic CETOP numerical algorithm, to retain all the capabilities the S-TORC modelling method has. Generation of design model involves selection of an optimal core representation which will result in a best estimate of the hot channel flow properties and a preparation of input describing the operating conditions and geometrical configuration of the core. The CETOP-D model presented here provides an additional simplification to the conservation equations due to the specific geometry of the model. A description of this simplification is included here together with an explanation on the method for generating enthalpy transport coefficients in CETOP-D.

4.1 Geometry of CETOP-D Design Model

The CETOP-D design model has a total of four thermal-hydraulic channels to model the open-core fluid phenomena. Figure 4.1 shows a typical layout of these channels. Channel 2 is a quadrant of the hottest assembly in the core and Channel 1 is an assembly which represents the average coolant conditions for the remaining portion of the core. The boundary between channels 1 and 2 is open for crossflow, but there is no turbulent mixing across the boundary. Turbulent mixing is only allowed within channel 2. The outer boundaries of the total geometry are assumed to be impermeable and adiabatic. The lumped Channel 2 includes channels 3 and 4. Channel 3 lumps the subchannels adjacent to the MDNBR hot channel 4. The location of the MDNBR channel is determined from a Detailed TORC analysis of a core. Channels 2' and 2" are discussed in Section 4.2.

The radial power factor and inlet flow factor for channel 1 in CETOP-D is always unity since this channel represents the average coolant conditions in the core. The Channel 2 radial power distribution is normally based upon a core average radial factor of unity. However, prior to providing input in CETOP-D, the Channel 2 radial power distribution is normalized so the Channel 2 power factor is one. This is performed in CETOP-D so the Channel 2 power can easily be adjusted to any value. Initially, the inlet flow factor in the CETOP-D hot assembly is equal to the hot assembly relative flow obtained from the inlet flow distribution. If necessary, the inlet flow factor is later adjusted in the CETOP-D model to yield conservative or accurate MDNBR predictions as compared to a Detailed TORC analysis for a given range of operating conditions.

4.2 Application of Transport Coefficients in the CETOP-D Model



4.3 Description of Input Parameters

A user's guide for CETOP-D, Version 2 is supplied in Appendix A. To provide more information on the preparation of the input parameters, the following terms are discussed.

4.3.1 Radial Power Distributions

The core radial power distribution is defined by C-E nucleonics codes in terms of a radial power factor, $F_R(i)$, for each fuel assembly. The radial power factor $F_R(i)$ is equal to:

$$F_R(i) = \frac{\text{power generated in fuel assembly } i}{\text{power generated in an average fuel assembly}} \quad (4.7)$$

Assuming power generated in an average fuel assembly is equal to unity, the following expression exists:

$$\sum_{i=1}^N F_R(i) = N \quad (4.8)$$

where N is the total number of assemblies in the core.

The radial power factor for each fuel rod is defined by:

$$f_R(i,j) = \frac{\text{power generated in fuel rod } j \text{ of assembly } i}{\text{power generated in an average fuel rod}} \quad (4.9)$$

For an assembly containing M rods, one expects:

$$\sum_{j=1}^M f_R(i,j) = M F_R(i) \quad (4.10)$$

The CETOP-D code is built to allow only one radial power factor for each flow channel, thus, for a channel containing n rods, the idea of effective radial power factor is used:

$$\hat{f}_R(i) = \frac{\sum_{j=1}^n \zeta_j f_{R(i,j)}}{\sum_{j=1}^n \zeta_j} \quad (4.11)$$

where ζ_j is the fraction of the rod j enclosed in channel i.

4.3.2 Axial Power Distributions

The fuel rod axial power distribution is characterized by the axial shape index (ASI), defined as:

$$ASI = \frac{\int_0^{L/2} F_Z(k) dZ - \int_{L/2}^L F_Z(k) dZ}{\int_0^L F_Z(k) dZ} \quad (4.12)$$

where the axial power factor at elevation k, $F_Z(k)$, satisfies the normalization condition:

$$\int_0^L F_Z(k) dZ = 1 \quad (4.13)$$

and L, dZ are total fuel length and axial length increment respectively.

The total heat flux supplied to channel i at elevation k is:

$$\phi_i = (\text{core average heat flux}) (\hat{f}_R(i)) (F_Z(k)) \quad (4.14)$$

4.3.3 Effective Rod Diameter

For a flow channel containing n rods of identical diameter d, the effective rod diameter defined by:

$$\hat{D}(i) = \sum_{j=1}^n \zeta_j d \quad (4.15)$$

is used to give effective heated perimeter in channel i. The following expression, derived from Eq's. (4.11) and (4.15), implies that equivalent energy is being received by channel i:

$$\hat{D}(i) \hat{f}_R(i) = d \sum_{j=1}^n \zeta_j f_R(i,j) \quad (4.16)$$

4.3.4 Engineering Factors

The CETOP-D model allows for engineering factors (as described in Reference 1) due to manufacturing tolerances. Application of such factors imposes additional conservatism on the core thermal margin. Conventionally, engineering factors are used as multipliers to effectively increase the radial peaking factors and diameters of rods surrounding the hot channel. Alternatively, statistical methods are applied to produce a slightly increased DNBR design limit, which is then input as parameter 85 (Appendix A).

The former method requires further explanation on the treatment of engineering factors:

(1) Heat Flux Factor (f_ϕ)

A slightly greater than unit heat flux factor f_ϕ , acting as a heat flux multiplier, tends to decrease DNBR in the following manner:

$$DNBR = \frac{CHF}{f_\phi \phi_i} < \frac{CHF}{\phi_i} \quad \text{for } f_\phi > 1 \quad (4.17)$$

where $\frac{CHF}{\phi_i}$ defines the DNBR before applying f_ϕ and ϕ_i is the local heat flux.

(2) Enthalpy Rise Factor (f_H) and Pitch and Bow Factor (f_p)

These factors are involved in the modification of the effective radial power factors and rod diameters for the fuel rods surrounding the hot channel as follows:

$$\hat{f}_R(4) = \frac{f_H f_p \sum_{j=1}^m \zeta_j f_R(4,j)}{f_H f_p \sum_{j=1}^m \zeta_j} = \frac{\sum_{j=1}^m \zeta_j f_R(4,j)}{\sum_{j=1}^m \zeta_j} \quad (4.18)$$

$$\hat{f}_R(3) = \frac{f_H \sum_{j=1}^m \zeta_j f_R(3,j) + \sum_{j=1}^n \zeta_j f_R(3,j)}{f_H \sum_{j=1}^m \zeta_j + \sum_{j=1}^n \zeta_j}$$

and

$$\hat{D}(4) = f_H f_P d \sum_{j=1}^m \zeta_j \quad (4.19)$$

$$\hat{D}(3) = d \left(f_H \sum_{j=1}^m \zeta_j + \sum_{j=1}^n \zeta_j \right) \quad (4.20)$$

where f_R 's and D 's are the modified effective radial power factors and rod diameters for channels 4 and 3, m is the number of rods on channel connection 4-3 and n is the number of rods []

Again, the inclusion of f_H and f_P in the core thermal margin prediction causes a net decrease in DNBR in addition to that described in Eq. (4.17).

5. THERMAL MARGIN ANALYSES USING CETOP-D

This section supports the CETOP-D model by comparing its predictions for a 16x16 assembly type C-E reactor (ANO-2) with those obtained from a detailed TORC analysis. Several operating conditions were arbitrarily selected for this demonstration; they are representative of, but not the complete set of conditions which would be considered for a normal DNB analysis.

5.1 Operating Ranges

The thermal margin model for 2815 Mwt ANO-2, Cycle 2 was developed for the following operating ranges:

Inlet Temperature	465 - 605°F
System pressure	1750 - 2400 psia
Primary system flow rate	193,200 - 386,400 gpm
Axial power distribution	-0.527 - +0.527 ASI

5.2 Detailed TORC Analysis of Sample Core

The detailed thermal margin analyses were performed for the sample core using the radial power distribution and detailed TORC model shown in Figures 5.1, 5.2, and 5.3. The axial power distributions are given in Figure 5.4. The core exit pressure and inlet flow distribution used in the analyses were based on flow model test results, given in Figures 5.5 and 5.6. The results of the detailed TORC analyses are given in Table 5.1.

5.3 Geometry of CETOP Design Model

The CETOP design model has a total of four thermal-hydraulic channels to model the open-core fluid phenomena. Figure 5.7 shows the layout of these channels. Channel 2 is a quadrant of the hottest assembly in the core (location 8) and Channel 1 is an assembly which represents the average coolant conditions for the remaining portion of the core. The boundary between channels 1 and 2 is open for crossflow; the remaining outer boundaries of channel 2 are assumed to be impermeable and adiabatic. Channel 2 includes channels 3 and 4. Channel 3 lumps the subchannels adjacent to the MDNBR hot channel 4.

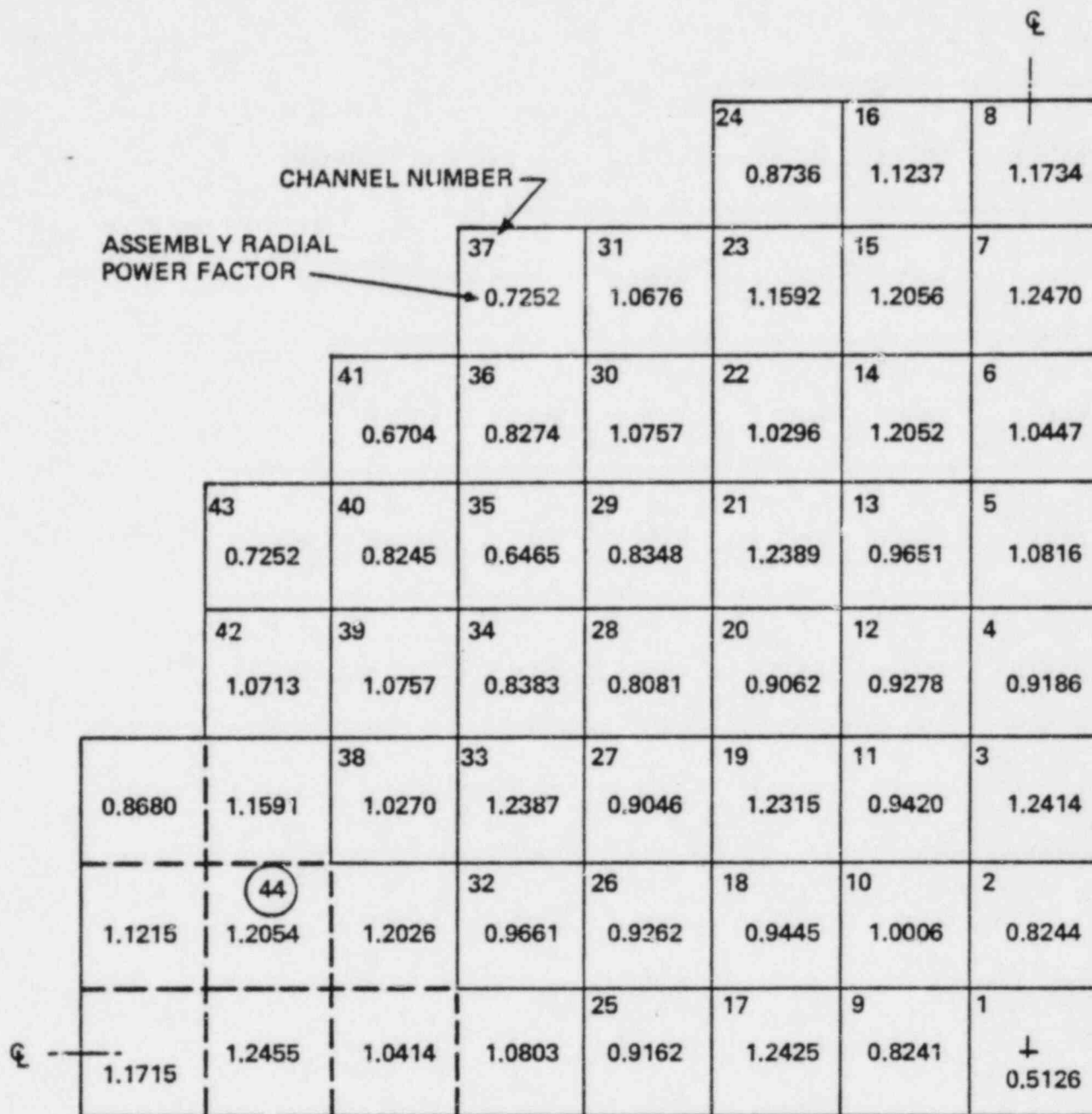
5.4 Comparison Between TORC and CETOP-D Predicted Results

The CETOP model described above was applied to the same cases as the detailed TORC analyses in section 5.2. The results from the CETOP model analyses are compared with those from the detailed analyses in Table 5.1. It was found that a constant inlet flow split providing a hot assembly inlet mass velocity of .80 of the core average value is appropriate for 4-pump operation so that MDNBR results predicted by the CETOP model are either conservative or accurate.

A similar procedure to that described above shows that a CETOP-D hot assembly flow factor of [] is appropriate for 3-pump operation.

5.5 Application of Uncertainties in CETOP-D

An allowance for the system parameter uncertainties in ANO-2 cycle 2 was derived statistically in Reference 6. This allowance has been incorporated into the design CETOP-D model in the form of a design MDNBR limit equal to 1.24, replacing the original design limit of 1.19.



NOTE: CIRCLED NUMBER DENOTES "LUMPED" CHANNEL

Figure 5.1
STAGE 1 TORC CHANNEL GEOMETRY FOR ANO-2, CYCLE 2

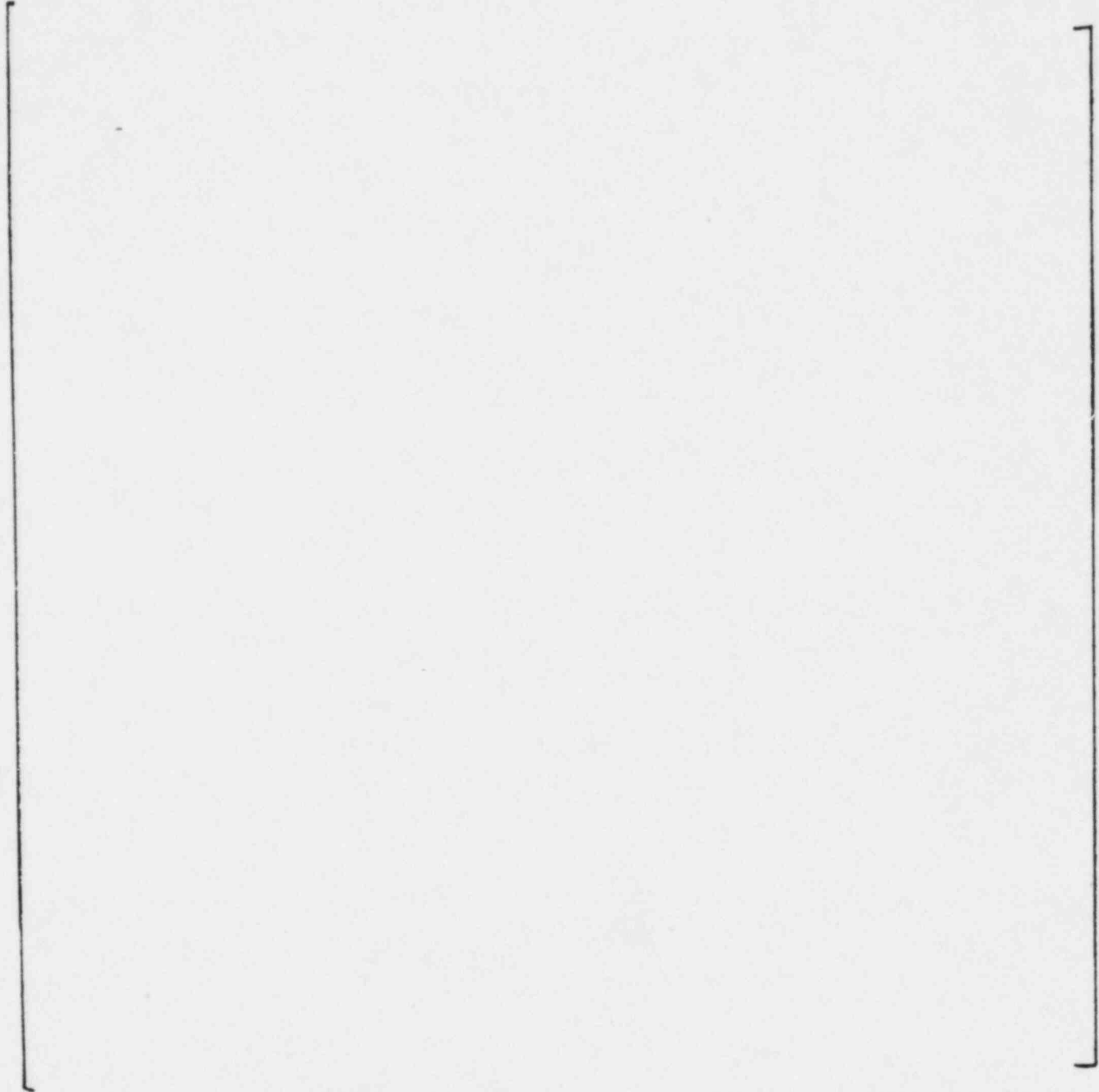


Figure 5.2
STAGE 2 TORC CHANNEL GEOMETRY FOR ANO-2, CYCLE 2, LOCATION 8

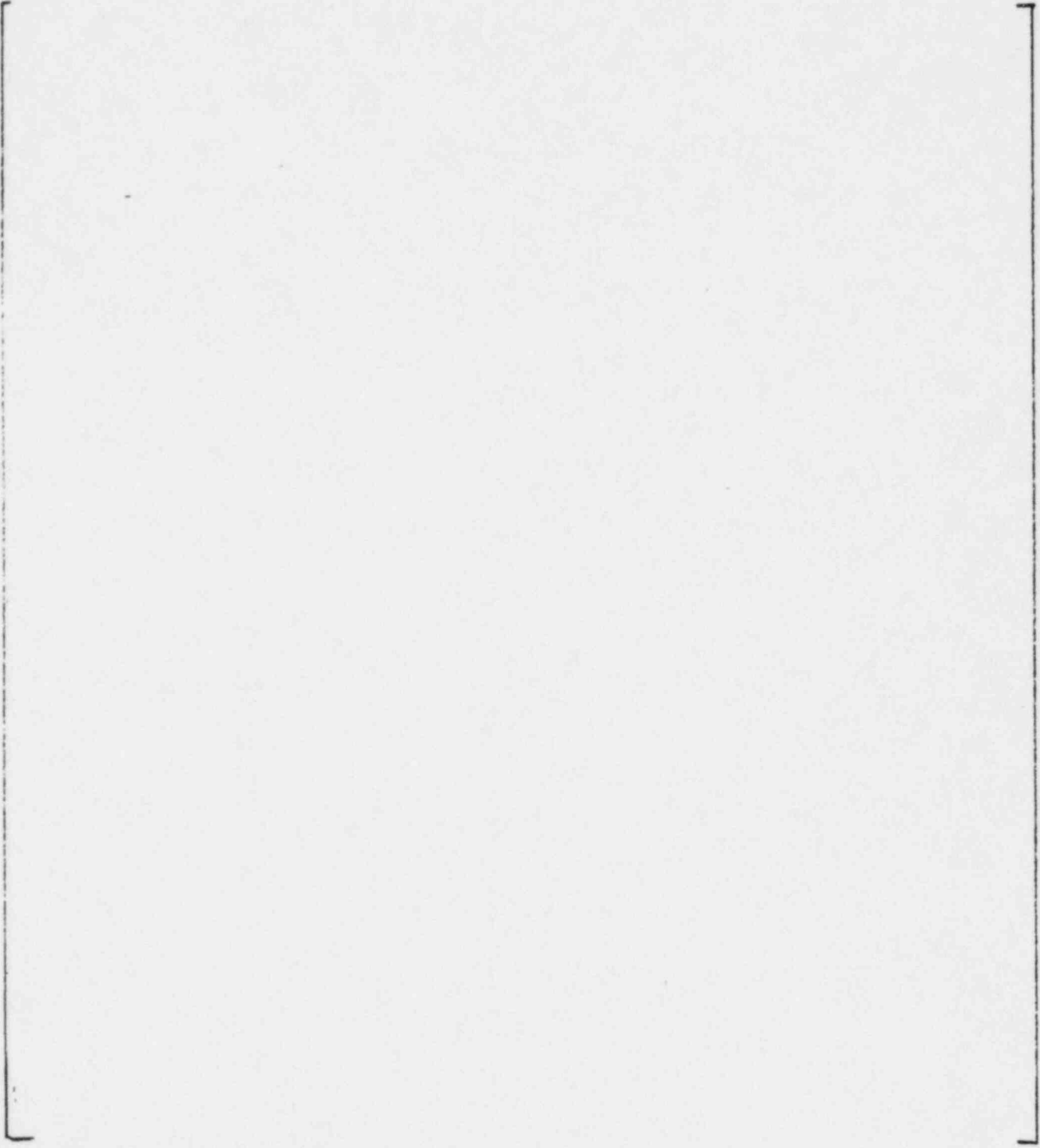


Figure 5.3
STAGE 3 TORC CHANNEL GEOMETRY FOR ANO-2, CYCLE 2

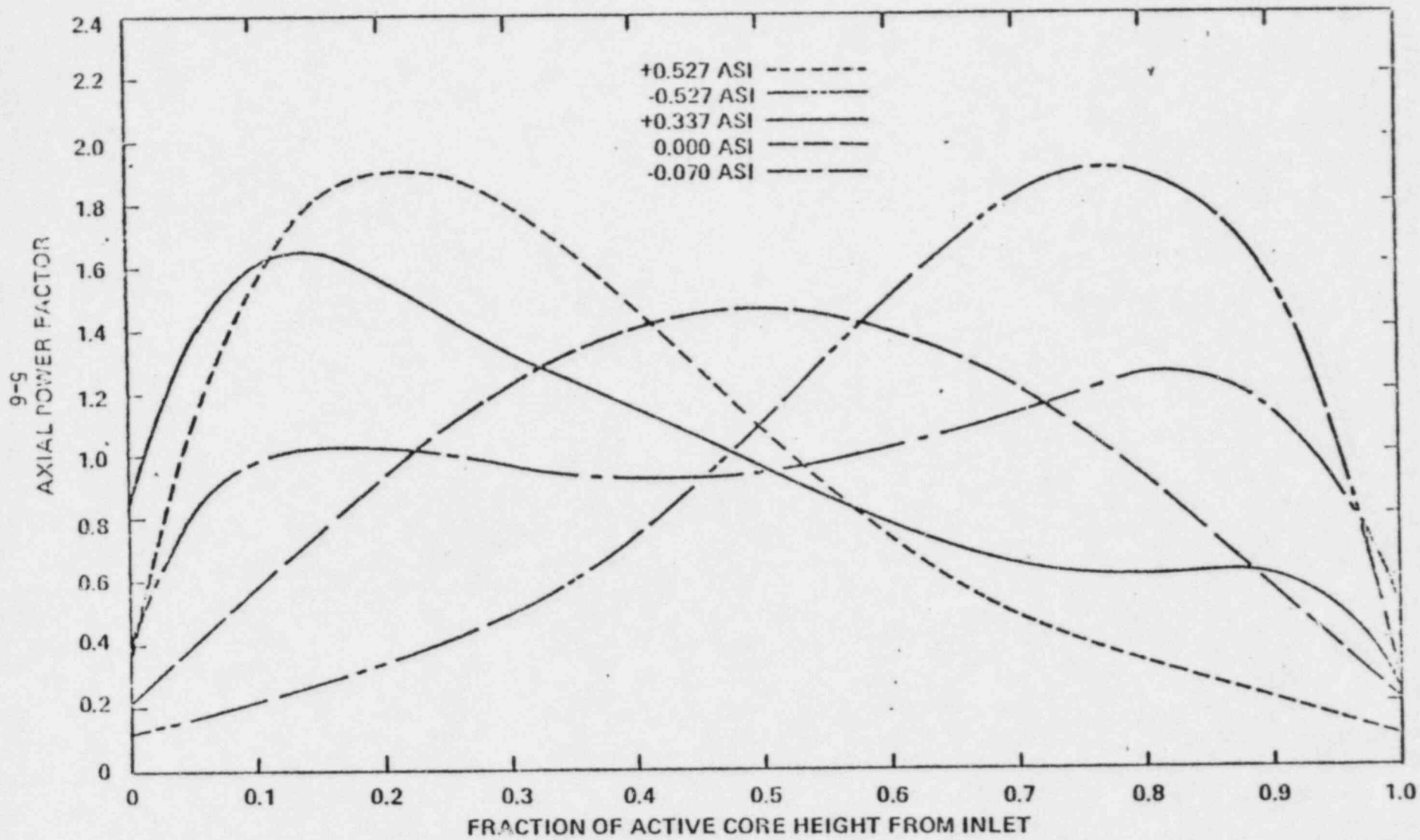


Figure 5.4
 AXIAL POWER DISTRIBUTIONS

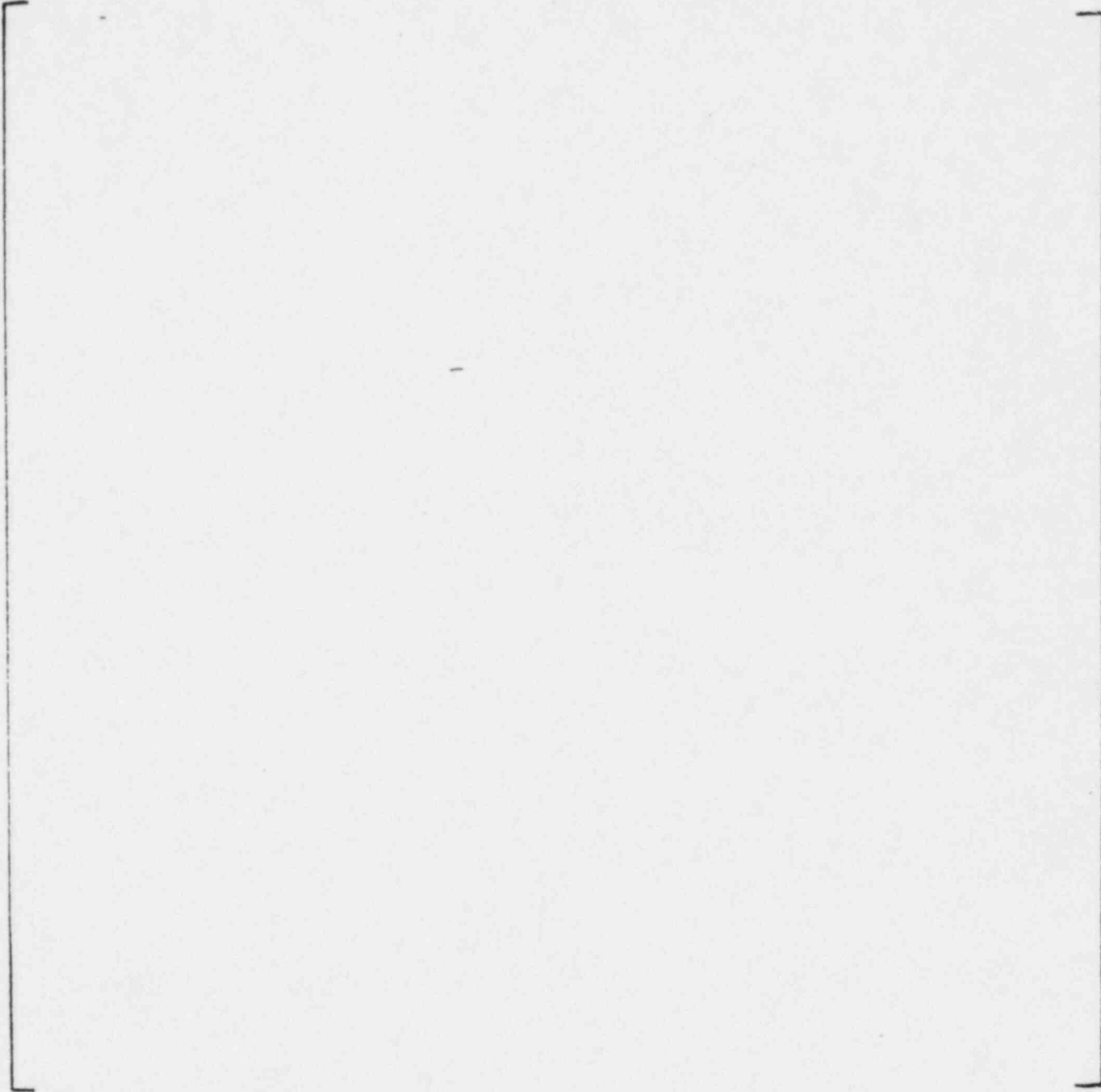


Figure 5.5
INLET FLOW DISTRIBUTION FOR ANO-2, CYCLE 2 4-PUMP OPERATION

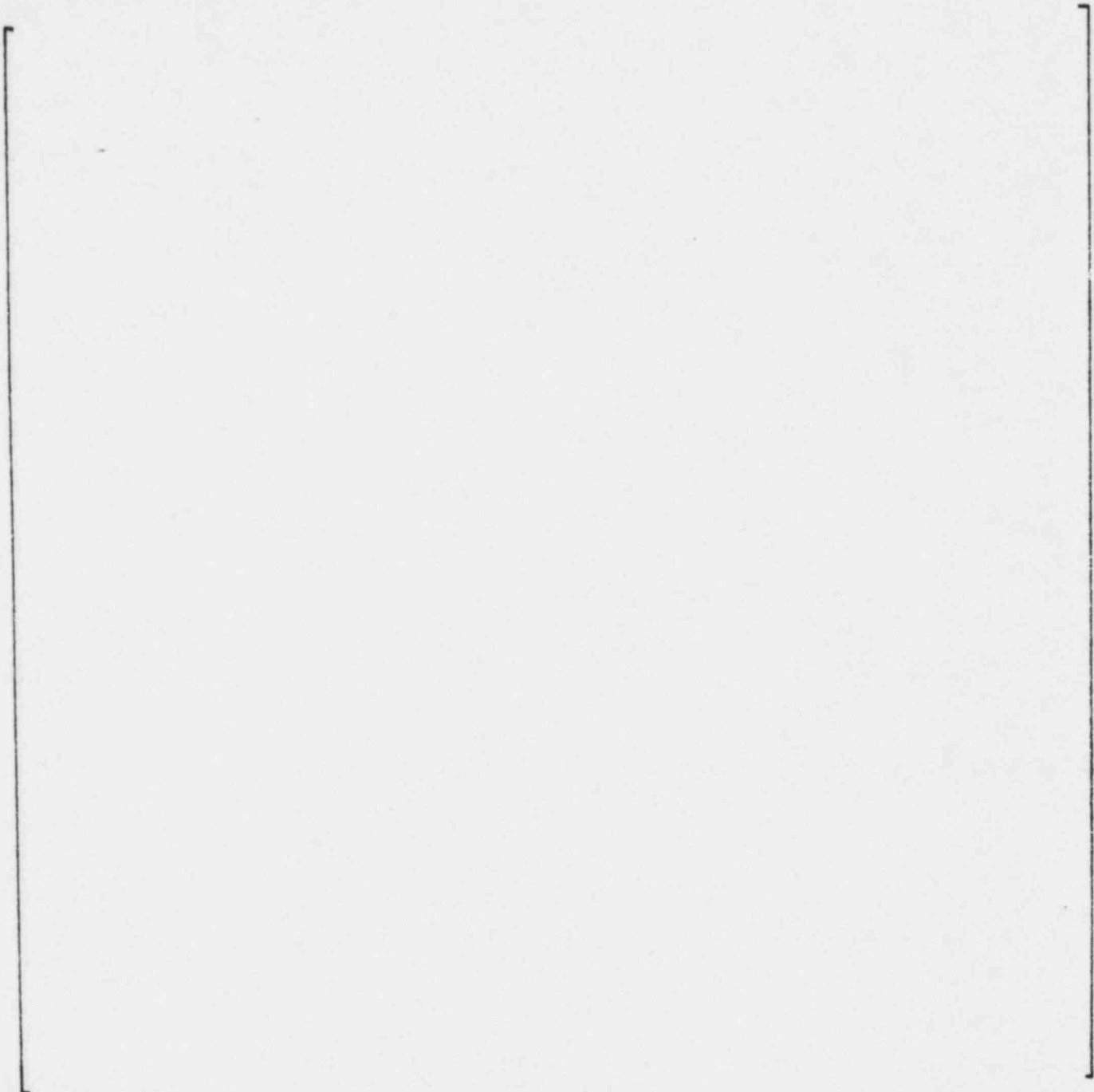


Figure 5.6
EXIT PRESSURE DISTRIBUTION FOR ANO-2, CYCLE 2 4-PUMP OPERATION

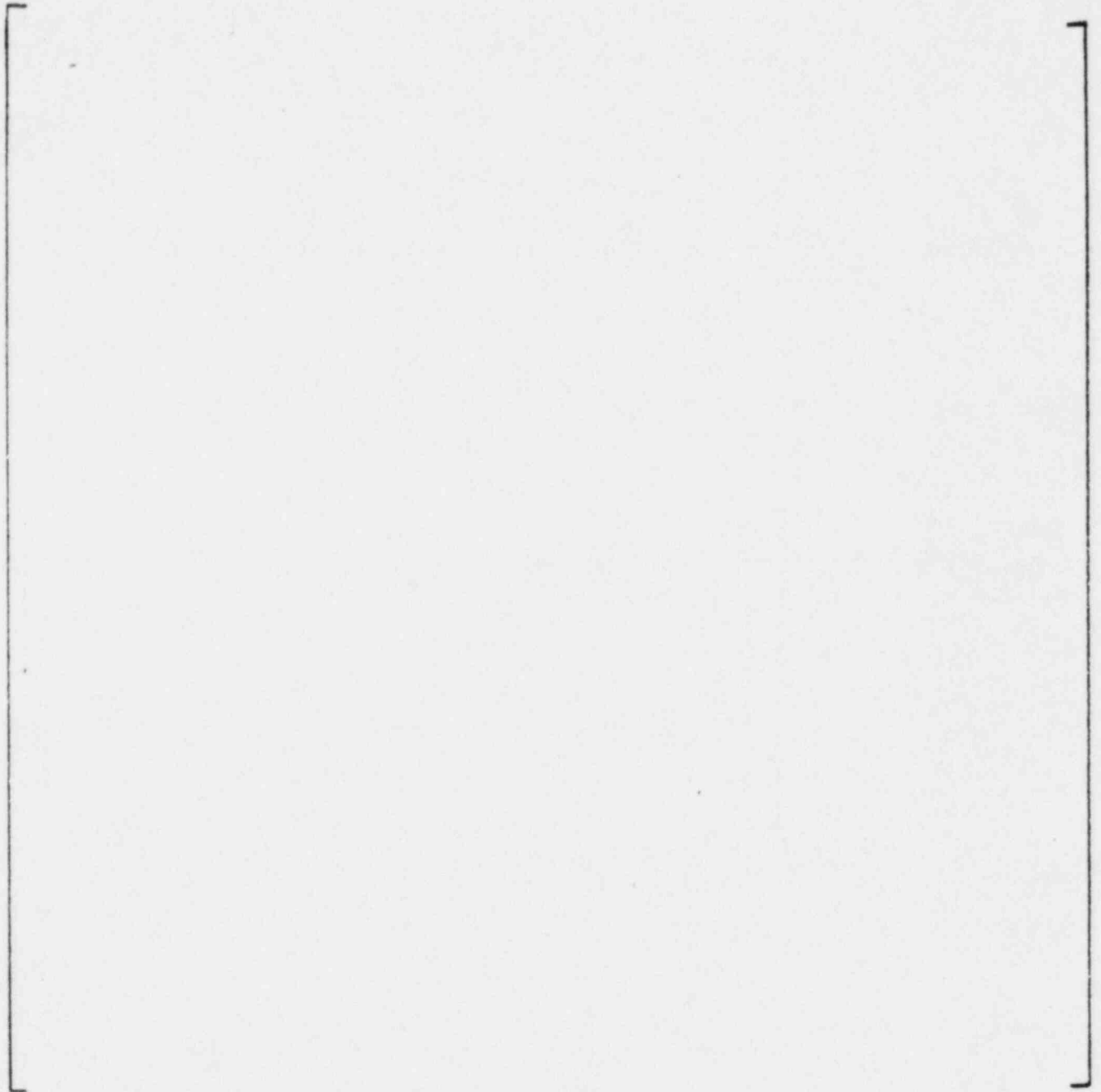


Figure 5.7
CETOP-D CHANNEL GEOMETRY FOR ANO-2, CYCLE 2
(CHANNEL 1 NOT SHOWN)

Operating Parameters					MDNBR		Quality at MDNBR		Axial Elev. of MDNBR (in)	
Pressure (psia)	Inlet Temp. (°F)	Core Avg. Mass Velocity ($\frac{10^6 \text{ lbm}}{\text{hr-ft}^2}$)	Core Avg. Heat Flux ($\frac{\text{Btu}}{\text{hr-ft}^2}$)	Axial Shape Index ASI	Detailed TORC	CETOP-D	Detailed TORC	CETOP-D	Detailed TORC	CETOP-D
					Relative Flow in Location 8 []	Inlet Flow Factor [] .80	Relative Flow in Location 8 []	Inlet Flow Factor [] .80		
2250	553.5	2.598	267437	+ .527	1.172	1.144	-.134	-.112	52.4	56.1
2250	553.5	2.598	312561	+ .337	1.169	1.066	.153	.169	142.2	142.2
2250	553.5	2.598	278307	+0.00	1.186	1.137	-.017	.020	108.5	116.0
2250	553.5	2.598	264238	-.070	1.169	1.135	.028	.039	138.4	138.5
2250	553.5	2.598	225343	-.527	1.195	1.164	-.076	.066	131.0	131.0
1750	605	1.407	122096	+ .527	1.172	1.155	.181	.194	71.1	74.8
1750	553.5	1.547	168322	+ .527	1.181	1.178	.073	.089	63.6	67.4
2400	605	2.868	227330	+ .527	1.209	1.181	-.069	-.051	52.4	56.1
1750	465	2.868	392894	+ .337	1.166	1.068	.108	.123	142.2	142.2
2400	465	1.724	314014	+ .337	1.140	1.048	.164	.143	142.2	142.2
2400	605	2.390	238744	+ .337	1.162	1.067	.203	.213	142.2	142.2
2400	605	1.434	120256	-.527	1.180	1.178	.064	.069	134.7	134.7
2400	553.5	1.562	162529	-.527	1.203	1.183	-.065	-.055	131.0	131.0

5-10

TABLE 5.1 COMPARISONS BETWEEN DETAILED TORC AND CETOP-D

6. CONCLUSION

CETOP-D, when benchmarked against Detailed TORC for ANO-2 cycle 2, has been shown to produce a conservative and accurate representation of the DNB margin in the core. Similar conclusions have been reached when CETOP-D results have been compared to TORC results for other C-E plants. CETOP-D models thus are appropriate substitutes for Design TORC models (S-TORC) specifically for ANO-2 cycle 2, and generally for applications in which the Design TORC methods have been approved (Reference 16).

7. REFERENCES

1. "TORC Code, A Computer Code for Determining the Thermal Margin of a Reactor Core", CENPD-161-P, July 1975.
2. Chiu, C., et al, "Enthalpy Transfer Between PWR Fuel Assemblies in Analysis by the Lumped Subchannel Model", Nuc. Eng. and Des., 53 (1979), p. 165-186.
3. Hetsroni, G., "Use of Hydraulic Models in Nuclear Reactor Design", Nuclear Science and Engineering, 28, 1967, pgs. 1-11.
4. Chiu, C.; Church, J. F., "Three Dimensional Lumped Subchannel Model and Prediction-Correction Numerical Method for Thermal Margin Analysis of PWR Cores", Combustion Eng. Inc., presented at Am. Nuc. Society Annual Meeting, Jan, 1979.
5. "TORC Code, Verification and Simplification Methods", CENPD 206-P, January, 1977.
6. "Statistical Combination of Uncertainties, Combination of System Parameter Uncertainties in Thermal Margin Analyses for Arkansas Nuclear One Unit 2", CEN-139 (A)-P, November, 1980.
7. McClintock, R.B.; Silvestri, G. J., "Formulations and Iterative Procedures and the Calculation of Properties of Steam", ASME, 1968.
8. McClintock, R.B.; Silvestri, G.J., "Some Improved Steam Property Calculation Procedures", ASME Publication 69-WA/PWR-2.
9. Dittus, F.W.; Boelter, L.M.K., University of California Pubs. Eng. 2, 1930, pg. 443.
10. Jens, W. H.; Lottes, P.A., Argonne National Laboratory Report, ANL-4627, May 1, 1951.
11. Sher, N.C.; Green, S. J., "Boiling Pressure Drop in Thin Rectangular Channels", Chem. Eng. Prog. Symposium Series, No. 23, Vol. 55, pgs. 61-73.
12. Martinelli, R.C. and Nelson, D.B.; Trans. Am. Soc. Mech. Engrs., 70, 1948 pg. 695.
13. Pyle, R.S., "STDY-3, A Program for the Thermal Analysis of a Pressurized Water Nuclear Reactor During Steady-State Operation", WAPD-TM-213, June 1960.
14. "CE Critical Heat Flux Correlation for CE Fuel Assemblies with Standard Spacer Grids", CENPD-162-P-A, September 1976.
15. Berringer, R.; Previti, G. and Tong, L.S., "Lateral Flow Simulation in an Open Lattice Core", ANS Transactions, Vol. 4, 1961, pgs. 45-46.

16. Letter dated 12/11/80, R. L. Tadesco (NRC) to A.E. Scherer (C-E), "Acceptance for Referencing of Topical Report CENPD-206(P), TORC Code Verification and Simplified Modeling Methods".
17. CEN-139(A)-P, "Responses to First Round Questions on the Statistical Combination of Uncertainties Program: CETOP-D Code Structure and Modeling Methods," March 1981. Transmitted to NRC by letter from D. C. Trimble (AP&L) to Director, NRC, July 15, 1981.
18. Robert A. Clark (NRC) to William Cavanaugh III (AP&L), "Operation of ANO-2 During Cycle 2," July 21, 1981 (Safety Evaluation and Amendment No. 26 to Facility Operating License No. NPF-6 for ANO-2).
19. CEN-157(A)-P, Amendment 1-P, "Response to Questions on Documents Supporting the ANO-2 Cycle 2 License Submittal," June 1981.

Appendix A CETOP-D VERSION 2 USER'S GUIDE

A.1 Control Cards

Code Access and Output Control Cards

A.2 Input Format

- 1) Read case control card, Format (I10, 70A1)

Case Number, I10

Alphanumeric information to identify case, 70A1

- 2) Read Relative Addresses and Corresponding Input Parameters,

Format (I1, I4, I5, 4E15.8)

N1: 0 or blank, continue to read in the next card. Otherwise any value in this location indicates end of input for the case. Successive cases can be performed by adding input after the last card of each case. The title card must be included for each case.

N2: Specifies the first relative address for data contained on this card.

N3: Specifies the last relative address for data contained on this card.

XLOC (N2): corresponding input parameters

thru

XLOC (N3): "

A.3 List of Input Parameters

Parameters	Relative Address	Units	Descriptions
GIN	1	million-lbm hr-ft ²	Core average inlet mass velocity, during core flow iteration ¹ this value is the initial guess.
XLOC(2)	2	million-Btu hr-ft ²	Core average heat flux, during core power iteration this value is the initial guess
TIN	3	°F	Core Inlet Temperature
PREF	4	PSIA	System Pressure
NXL	5	None	Use 0.0 to include the capability for adjusting the initial guess during "iteration" [*] , so the number of iterations may be reduced. Specify 1.0 to not use the capability.
NPOWER ¹	6		Use 1.0 to print more parameters during iteration in the event of convergence problem. Specify 0.0 to not print.
	7-25	None	For future work
GRJDXL(J) J=1, NGRID	26-(25+NGRID)	None	Relative Grid Location (X/Z), where X is distance from bottom of active core to top of spacer grid, Z is the total channel axial length (relative address 77).
	(25+NGRID+1)-45	None	For future work
A(I) I=1,4	46-49	ft ²	Flow Area for Channel I
PERIM(I) I=1,4	50-53	ft	Wetted Perimeter for Channel I
HPERIM(I) I=1,4	54-57	ft	Heated Perimeter for Channel I

Parameters superscripted with 1 are not included in CETOP-D Version 1.

*The term "iteration" can be defined as either iteration on core power, core flow or on Channel 2 radial peaking factors

Parameters	Relative Address	Units	Descriptions
FR	58	None	Maximum rod radial peaking factor wanted for Channel 2. During radial peaking factor iteration this value is the initial guess.
PIPB	59	None	Ratio of the maximum rod radial peaking factor of Channel 2 to the Channel 2 average radial factor. This ratio is based upon a power distribution normalized to the core
RADIM1	60	None	Effective radial peaking factor for Channel 1
RADIAL(I) I=2,4	61-63	None	Effective normalized radial peaking factor for Channel I (normalized to the Channel 2 average radial factor in the core power distribution, if this is done correctly RADIAL(2) will always be 1). A channel normalized radial peaking factor is determined by multiplying the normalized radial peaks in the channel by the corresponding rod fractions depositing heat to the channel.
D(I) I=1,4	64-67	ft	Effective rod diameter for Channel I, determined by multiplying the rod diameter with the rod fractions depositing heat to the Channel (assuming diameter of all rods in Channel are the same).
GAP(I) I=1,3	68-70	ft	Gap width available for crossflow between Channel I and Channel I+1. []
NDX	71	None	Number of axial nodal sections in model, maximum of 49 (recommend 40)
NCHANL	72	None	Number of Channels (always 4)
NGRID	73	None	Number of spacer grids (maximum number of 12)
ITMAX	74	None	Maximum number of iterations (recommend 10). Insert 0.0 for no iteration then a MDNBR will be calculated for the input core power, core flow and channel 2 radial peaking factor.

Parameters	Relative Address	Units	Descriptions
PDES	75	PSIA	Reference pressure at which the core average mass flux is specified. If the core inlet mass flux (GIN) is specified at (TIN,PREF) then PDES can be set to 0.0. If not, the code will correct the inlet mass flux to TIN and PREF by using PDES and TDES as reference conditions.
TDES	76	$^{\circ}\text{F}$	Reference temperature at which the core average mass flux is specified. Can be set to 0.0 for the same reasoning stated above.
Z	77	ft	Total channel axial length, where active length of fuel is corrected for axial densification.
DEMATX	78	ft	Hydraulic diameter of a regular matrix channel for use in calculating MDNBR in hot channel
QFPC	79	None	Fraction of power generated in the fuel rod plus clad
SKECDK	80	None	Engineering heat flux factor.
FSPLIT	81	None	Inlet flow factor for Channels 2, 3, 4
DDH(1)	82	ft	[
DDH(2)	83	ft	Heated hydraulic diameter of channel 4.
COMIX	84	ft^{-1}	Parameter used in the turbulent mixing correlation, determined by taking the ratio of the number of subchannels along one side of a complete fuel bundle to the gap width on that side.
DDNBR	85	None	Design limit on DNBR for CE-1 CHF correlation

Parameters	Relative Address	Units	Descriptions
DNBRCO	86	None	Initial value of the DNBR derivative with respect power during core power iteration [] and with respect to flow during core flow iteration [].
DNBRTOL	87	None	Tolerance on DNBR limit.
QUALMX	88	None	Maximum acceptable coolant quality at MDNBR location.
QUALCO	89	None	Initial value of the quality derivative with respect power during core power iteration [] and with respect to flow during core flow iteration [].
QUALTOL	90	None	Tolerance on quality limit.
AHDAF	91	None	Ratio of core heat transfer area to flow area, used for specifying a core saturation limit during overpower iteration. Insert 0.0 for not using the limit.
HTFLXTL	92	None	Convergence window tolerance on the ratio of the present guess to the previous one during "iteration". This tolerance is used to reduce oscillation during iteration.
DTIME	93	Sec.	CESEC time, this parameter is printed in the output when the CESEC code is linked with CETOP-D.
CH(2)	94	None	Average enthalpy transport coefficient in the total channel axial length between CHs. 2 and 3. Insert 0.0 for CETOP to self-generate the transport coefficients.
AMATX	95	ft ²	[]
GAPT	96	ft	

Parameters	Relative Address	Units	Descriptions
HC	97	None	[]
FSPLIT1	98	None	Inlet flow factor for Channel 1
NX	99	None	Use 0.0 to not print enthalpy transport coefficient factors and enthalpy distribution in channels. Use 1.0 to specify information.
NY	100	None	Use 0.0 for not using the relative locations of the axial power factors as long as the axial power factors are input at the node interfaces. Use 1.0 to specify locations.
NZ	101	None	Use 0.0 to write output on tape 8 and print one line of information, use 1.0 to write output on tape 8 and print all output.
XLOC(102)	102	million-BTU hr-ft ²	Core average heat flux at 100% power, includes heat generated from rods and coolant. Fuel rods are corrected for axial densification.
XLOC(103)	103	None	QUIX file case number. The QUIX code is used in Physics to generate axial power shapes.
HRAD.	104	None	Option to "iterate" on the following until the design limit on DNBR is reached. 0.0: Iterate on core power, if address (74) is 0.0 there is no iteration. 1.0: To iterate on channel 2 radial peaking factor. When this option is used the core heat flux in Channel 1 remains constant while all the Channel 2 radial peaking factors vary by the same multiplier until the DNB limit is reached. 2.0: Iterate on core flow ¹

Parameters	Relative Address	Units	Descriptions
NZZ	105	None	Use 0.0 to not print CESEC time (DTIME) Specify 1.0 to print.
GRKIJ(J) J=1,NGRID	106-117	None	Option to input different spacer grid types with the corresponding loss coefficient equations. 0.0 Normal grid with built in loss coefficient 1.0 Type 1 grid with coefficient equation = $CAA(1) + CBB(1) * (Re)^{CCC(1)}$ 2.0 Type 2 grid = $CAA(2) + CBB(2) * (Re)^{CCC(2)}$ 3.0 Type 3 grid = $CAA(3) + CBB(3) * (Re)^{CCC(3)}$
CAA(1)	118	None	Constant for Type 1 grid equation
CBB(1)	119	None	Constant for Type 1 grid equation
CCC(1)	120	None	Constant for Type 1 grid equation
CAA(2)	121	None	Constant for Type 2 grid equation
CBB(2)	122	None	Constant for Type 2 grid equation
CC(2)	123	None	Constant for Type 2 grid equation
CAA(3)	124	None	Constant for Type 3 grid equation
CBB(3)	125	None	Constant for Type 3 grid equation
CCC(3)	126	None	Constant for Type 3 grid equation
	127-128	None	Reserved for additional input

Parameters	Relative Address	Units	Descriptions
RAA2	129	None	<div style="border: 1px solid black; padding: 10px;"> <p>For Future Work</p> <p>Number of axial power factors (Recommend 41)</p> <p>Relative locations (X/Z) of the axial power factors. If NY = 0.0 this input is not needed.</p> <p>Normalized axial power factors</p> <p>Specify 1.0 to use the capability to change the hot assembly flow factor for different regions of operating space. Specify 0.0 to not use the capability. If 1.0 is specified, the following additional input is required.</p> <p>Number of operating space regions (maximum is 5)</p> </div>
RAA22	130	None	
GAP2P	131	ft	
GAP22	132	ft	
A2P	133	ft ²	
A22	134	ft ²	
DD2P	135	ft	
DD22	136	ft	
NDXPZ	137 - 139	None	
XXL(J) J=1,NDXPZ	141 - 190	None	
AXIAZ(J) J=1,NDXPZ	191 - 240	None	
NFIND ¹	241	None	
NREG ¹	242	None	

Parameters	Relative Address	Units	Descriptions
REFLO ¹	243	$\frac{\text{g.p.m.}}{\text{ft}^2}$	100% design core flow rate in g.p.m. divided by core flow area
FF(J) ¹ J=1,NREG	244-248	None	Channels 2,3, and 4 inlet flow factor for each region of operating space. (Referred to as hot assembly flow factor)
DOJ=1,NREG where: K=(J-1)*12	Provide for each region of operating space Ranges on fraction of 100% design core flow, inlet temperature system pressure, and ASI: 249 - 308		
IBF(J) ¹	(249+K)	None	Types of inequalities applied to limits of the design core flow range 1: lower limit \leq core flow \leq upper limit 2: lower limit $<$ core flow \leq upper limit 3: lower limit \leq core flow $<$ upper limit 4: lower limit $<$ core flow $<$ upper limit
BFL(J) ¹	(250+K)	None	Lower limit fraction of 100% design core flow rate.
BFR(J) ¹	(251+K)	None	Upper limit fraction of 100% design core flow rate.

Parameters	Relative Address	Units	Descriptions
ITI(J) ¹	(252+K)	None	Types of inequalities applied to limits of the inlet temperature range, same as IBF.
TIL(J) ¹	(253+K)	°F	Lower limit inlet temperature
TIR(J) ¹	(254+K)	°F	Upper limit inlet temperature
IPS(J) ¹	(255+K)	None	Types of inequalities applied to limits of the system pressure range, same as IBF.
PSL(J) ¹	(256+K)	psia	Lower limit system pressure
PSR(J) ¹	(257+K)	psia	Upper limit system pressure
IAS(J) ¹	(258+K)	None	Types of inequalities applied to limits of the A.S.I. range
ASL(J) ¹	(259+K)	None	Lower limit A.S.I. range
ASR(J) ¹	(260+K)	None	Upper limit A.S.I. range

A.4 Sample Input and Output

A sample input and output are attached using the model given in Figure 5.7. A definition of the titles used in the output is shown below.

CASE = CETOP-D case number

NH = Enthalpy transport coefficient at each node

H1 = Enthalpy in Channel 1

H2 = Enthalpy in Channel 2

[]

H3 = Enthalpy in Channel 3

H4 = Enthalpy in Channel 4

QDBL = core average heat flux, represents total heat generated from rods and coolant, where fuel rods are corrected (for axial densification) Btu/hr-ft².

- for core power iteration, the heat flux at the end of the last iteration is printed.

- For no iteration, core flow iteration, and radial peaking factor iteration, the heat flux given in the input XLOC(2) is printed.

POLR = for core power iteration, the ratio of the core average heat flux at the end of last iteration to the core average heat flux at 100% power is printed.

For no iteration, core flow iteration, and radial peaking factor iteration the ratio of XLOC(2) to the heat flux at 100% power is printed.

TIN = Inlet temperature, °F

PIN = System pressure, psia

GAVG = Core average mass velocity (10⁶ lb/hr-ft²)

- for core flow iteration the mass velocity at the end of the last iteration is printed.

ASI = Calculated axial shape index based upon axial shape factors input.

NRAD = 0, core power iteration, if address (74) is 0.0 there is no iteration
 1, Channel 2 radial peaking factor iteration
 2, core flow iteration

P1MAX = maximum rod radial peaking factor in Channel 2
 - for radial peaking factor iteration the max. peak at the end of the last iteration is printed.

DNB-N = hot channel MNDNR at last iteration
 X-N = coolant quality at location of DNB-N
 DNB-1 = hot channel MDNBR at first iteration
 X-1 = coolant quality at location of DNB-1

QUIX = QUIX file case number
 ITER = Number of "iterations"
 IEND = Specifies what type of limit or problem was encountered during "iteration".
 1 = MDNBR limit
 2 = maximum coolant quality limit
 3 = no additional iteration is needed because the ratio of the present guess to the previous one is within the window tolerance HTFLXTL, address 92.
 4 = core saturation limit
 5 = iteration has terminated because the maximum number of iterations has been reached.
 6 = the new guess produced by the code during iteration falls below zero. This may occur if the derivative on DNBR and Quality are not close to the actual values.

ATR = Average enthalpy transport coefficient over the total channel axial length.

HCH = MDNBR hot channel number, if 3 is printed this means [

MNOD = MDNBR node location

CESEC TIME = This parameter is printed in the output when the CESEC code is linked with CETOP-D.

FSPLIT = this is the inlet flow factor (in channels 2, 3, 4) chosen by the code for operating conditions specified in the input. This value is printed when the capability for changing the inlet flow factor for different regions of operating space is used. The following parameters are also printed to show that calculated fraction of 100% design core flow is within the operating space given in the input.

GAN = the calculated fraction of 100% design core flow

GIN = the calculated core average mass velocity, lb/sec-ft²

VIN = inlet coolant specific volume, ft³/lbm

Appendix B Sample CETOP-D Input/Output

870 AMU-2 CYCLE 2 & PUMP (P, NOMINAL (-,070431))

1	42,59800	.189456	.55315	.2250
26	29,0206	.1119	.2069	.3019
30	33,3969	.0919	.5869	.6818
34	36,7768	.0717	.9567	
46	49,25060	.06266	.002925	.001215
50	5324,883	6,221	.332	.12311
54	5722,80	5,90	.2795	.08529
58	611,4912	1,0940	1,0000	1,0
62	651,05610	1,07210		
64	677,13067	1,0782	.08898	.027135
68	70,086166	1,0250	.04051	
71	7440,	4,	11,	10,
75	760,	0,		
77	8012,4750	.0392825	.975	1,00000
81	84,800	0,00000	.05702	.92,8430
85	881,240	-.4	.005	.250
89	925,	.005	1133,38	1,001
94	970,00	0,000000	0,0000	0,0000
98	1011,000	1,	1,	1,
102	105,189456	0,0	0,0	1,
106	1091,	1,	1,	1,
110	1131,	1,	1,	1,
114	1161,	1,	1,	
116	120,59	0,	0,	
129	1321,04200	1,02508	.18518	.26118
133	136,007342	.0100956	.213436	.311811
140	14041,			
141	1440,000	.0375	.0625	.0875
145	148,1125	.1375	.1625	.1875
149	152,2125	.2375	.2625	.2875
153	156,3125	.3375	.3625	.3875
157	160,4125	.4375	.4625	.4875
161	164,5125	.5375	.5625	.5875
165	168,6125	.6375	.6625	.6875
169	172,7125	.7375	.7625	.7875
173	176,8125	.8375	.8625	.8875
177	180,9125	.9375	.9625	.9875
181	1811,000			
191	194,3900	.7200	.8750	.9600
195	1981,005	1,030	1,030	1,027
199	2021,020	1,005	.997	.9750
203	206,9600	.9450	.9350	.9300
207	210,9300	.9300	.9300	.9350
211	214,9500	.9650	.9850	1,005
215	2181,025	1,050	1,080	1,110
219	2221,140	1,175	1,205	1,235
223	2261,255	1,260	1,240	1,185
227	2301,110	.9950	.8250	.5700
231	231,5700			
1 93	9310,			

ANO-2 CYCLE 2 4 PUMP OP. NOMINAL (-.070A81)

CASE# 470

NODE	H1	H4	H3	[]	[]	H2	H1
1	1.1727	551.5501	551.5501	551.5501	551.5501	551.5501	551.5501
2	1.3163	553.5076	554.1767	554.0430	554.1385	554.0007	552.9154
3	1.6237	556.2990	557.7566	557.5010	557.6989	557.3443	554.8984
4	1.9235	559.7598	562.0853	561.7308	562.0216	561.4088	557.3120
5	2.3653	563.6315	566.7935	566.3802	566.7398	565.8284	559.9641
6	3.2767	567.7150	571.5967	571.1689	571.5651	570.2345	562.7585
7	4.2971	571.9581	576.3144	575.9153	576.3058	574.6546	565.6296
8	5.3729	576.1921	581.0518	580.6942	581.0516	579.1784	568.5035
9	7.1382	580.4507	585.7532	585.4499	585.7603	583.6610	571.3658
10	10.6657	584.7302	590.3713	590.1322	590.3829	587.9582	574.2250
11	17.2421	588.9884	594.7808	594.6136	594.7824	592.1221	577.0463
12	29.2763	593.1764	599.1820	599.0774	599.1554	596.3681	579.8410
13	80.5977	597.3026	603.4956	603.4505	603.4391	600.5213	582.5809
14	-181.1368	601.4012	607.7186	607.7288	607.6298	604.5006	585.2844
15	-51.1700	605.4614	611.7784	611.8378	611.6426	608.3746	587.9479
16	-34.6195	609.4520	615.8309	615.9282	615.6387	612.3082	590.5841
17	-28.6254	613.4195	619.8601	619.9367	619.6117	616.1513	593.2095
18	-25.8889	617.3993	623.8200	623.9170	623.5082	619.9696	595.8361
19	-24.7725	621.3533	627.8159	627.9146	627.4379	623.8606	598.4632
20	-24.1543	625.3098	631.8214	631.9192	631.3835	627.7527	601.0906
21	-25.0955	629.2889	635.8559	636.0253	635.3571	631.6275	603.7336
22	-25.8620	633.3317	639.8971	640.0505	639.3325	635.5520	606.4197
23	-29.8371	637.4074	644.0522	644.2040	643.4227	639.5925	609.1490
24	-32.3336	641.5714	648.3161	648.4599	647.6327	643.7212	611.8394
25	-36.4057	645.8265	652.6931	652.8160	651.9561	647.9356	614.7859
26	-44.1356	650.1614	657.0964	657.2398	656.2962	652.2410	617.6886
27	-55.2213	654.5892	661.6733	661.7571	660.8175	656.6847	620.6761
28	-62.5767	659.1677	666.4139	666.4783	665.5154	661.2311	623.7516
29	-77.5855	663.8874	671.3264	671.3982	670.3809	665.9326	626.9048
30	-127.9151	668.7257	676.3016	676.3188	675.2913	670.7777	630.1362
31	-224.5382	673.7161	681.5153	681.5428	680.4521	675.7979	633.4916
32	-264.9584	678.8815	686.9046	686.9274	685.8027	680.9748	636.9319
33	-574.4459	684.1995	692.4733	692.4857	691.3226	686.2870	640.4337
34	505.7651	689.6074	698.0369	698.0278	696.8152	691.7038	643.9724
35	884.6285	695.0635	703.7108	703.6911	702.4315	697.1713	647.5649
36	273.6208	700.4696	709.4922	709.4674	708.1530	702.5746	651.0413
37	608.2240	705.7172	715.0945	715.0806	713.6834	707.8185	654.5092
38	-72.2346	710.8620	720.3102	720.4017	718.9033	712.8298	657.8452
39	-36.9692	715.6822	725.0152	725.2071	723.5895	717.3938	660.8090
40	-25.9911	719.9040	728.8961	729.1790	727.4215	721.2137	663.2326
41	-20.2303	723.1447	731.4430	731.8049	729.8819	723.8697	664.8851

CASE 470 DNL PWR TIN PIN G AVG ASI NRAD PIMAX [] X-N DNH-1 X-1 JUIX IER IEND ATH HCH MNUD
 470 254068. 1.3431 553.5 2250. 2.59800 -.06825 0 1.4912 [] .0229 2.1806 -.0872 0. 4 1 11.2 0 38
 CASE SEC TIME = 10.00